Life-cycle-related gene expression patterns in the brown algae

Pélagie Ratchinski[1], Olivier Godfroy[2], Benjamin Noel[3], Jean-Marc Aury[3], J. Mark Cock[1,*]

[1]Sorbonne Université, CNRS, Algal Genetics Group, Integrative Biology of Marine Models Laboratory, Station Biologique de Roscoff, Roscoff, France
[2]Sorbonne Université, CNRS, CMAR, Integrative Biology of Marine Models Laboratory, Station Biologique de Roscoff, Roscoff, France
[3]Génomique Métabolique, Genoscope, Institut François Jacob, CEA, CNRS, Université Evry, Université Paris-Saclay, Evry 91057, France
*Corresponding author. E-mail address: cock@sb-roscoff.fr (J.M. Cock)

Keywords: brown algae, early development, *Dictyota dichotoma, Ectocarpus* species 7, gene clustering, life cycle, seaweed, transcriptomics

Abstract

Brown algae are important primary constituents of marine coastal ecosystems, characterised by complex life cycles and various levels of complex multicellular development. However, the molecular processes that underlie development and life cycle progression in the brown algae remain poorly understood. In this study, pairwise comparisons of gametophyte and sporophyte transcriptomes across ten diverse brown algal species showed that the total number of genes exhibiting generation-biased or generation-specific expression in each species was correlated with the degree of dimorphism between life cycle generations. However, analysis of gene ontology terms assigned to the generation-biased/generation-specific genes indicated that each generation (i.e. the sporophyte and the gametophyte) also has characteristic broad life-cycle-related features that have been conserved during evolution. A more detailed analysis of *Ectocarpus* species 7, identified progressive transcriptome changes over its entire life cycle with a particularly marked change in transcriptome composition during the first day of sporophyte development, characterised by downregulation of flagellar and transcription factor genes and upregulation of a subset of translation genes. Comparison with a similar transcriptomic time series for the evolutionarily-distant (about 250 My) brown alga *Dictyota dichotoma* indicated considerable conservation of co-expressed gene modules between the two species, particularly for modules that were enriched in genes assigned to evolutionarily-conserved functional categories. This study therefore identified broad life-cycle- and development-related patterns of gene expression that are conserved across the brown algae.

Introduction

Brown algae are major primary components of diverse and widespread coastal ecosystems, often forming extensive underwater forests (Bringloe *et al.*, 2020; Eger *et al.*, 2023). The group includes large (up to 50 metres) multicellular organisms that rival many land plant species in complexity. From a developmental point of view, brown algae are particularly interesting because they evolved complex multicellularity independently of land plants and animals (Cock *et al.*, 2010). Taxonomically, these seaweeds are grouped into the class Phaeophyceae, which is a major taxon within the stramenopiles, and therefore very distant, phylogenetically, from the Archaeplastida and the Opisthokonta lineages that gave rise to land plants and animals, respectively. Consequently, brown algae represent interesting alternative systems to investigate the evolution and molecular bases of developmental processes.

Most brown algae have haploid-diploid life cycles involving an alternation between two independent multicellular generations, the sporophyte and the gametophyte (Cock *et al.*, 2014). These seaweeds are therefore capable of deploying two different multicellular developmental programs, each at the

appropriate stage of their complex life cycles. The ecological functions of brown algal haploid-diploid life cycles can be difficult to study, particularly when one of the generations is microscopic. However, there is evidence, in kelps for example, that microscopic stages (gametophytes, but possibly also very young sporophyte stages) may have a survival function, allowing a population to persist when the macroscopic sporophyte stage is not present (Carney and Edwards, 2006). A study of populations of filamentous brown algae of the genus *Ectocarpus* in the field indicated that gametophytes grew epiphytically on the brown alga *Scytosiphon promiscuus* (then classified taxonomically as *Scytosiphon lomentaria*) in the spring, whereas sporophytes grew throughout the year on abiotic substrata. These observations indicate that the sporophyte may be the most important generation for persistence of the population in this genus (Couceiro *et al.*, 2015). Note, however, that a principally asexual population of *Ectocarpus siliculosus* located at a second site inhabited both epiphytic and epilithic niches indicating that the relationship between life cycle generation and niche may be complex (Couceiro *et al.*, 2015). The phenology of the brown alga *D. dichotoma* also appears to be complex with, for example, overlapping generations and sporophytes and gametophytes reported to occur simultaneously (Tronholm *et al.*, 2008).

The relative sizes of the two life cycle generations varies considerably across brown algae, with either the sporophyte or the gametophyte being the largest generation (dimorphism) or the two generations having very similar sizes and morphologies (isomorphy). Transitions between life cycles with different degrees of dimorphism have occurred frequently during the evolution of the brown algae (Cock *et al.*, 2014). Variations on this central sexual life cycle have been observed in culture for several species and these variations can provide insights into the mechanisms that control life cycle progression. For example, if *Ectocarpus* gametes fail to fuse with a gamete of the opposite sex to form a zygote, they are often capable of germinating parthenogenetically to produce a haploid partheno-sporophyte that is morphologically and functionally indistinguishable from a diploid sporophyte (Müller, 1967). The existence of these haploid sporophytes indicates that life cycle generation identity is not determined by ploidy in this species and is therefore presumably under genetic control.

The occurrence of two multicellular generations during the life cycles of most brown algae allows genetic screens to be carried out for mutations that cause switching between the development programs of the two generations, i.e. mutations that lead to deployment of the incorrect program at a specific point in the life cycle (Coelho and Cock, 2020). Using this approach, two three-amino-acid-loop-extension (TALE) homeodomain transcription factor (HD TF) genes, *OUROBOROS (ORO)* or *SAMSARA (SAM)*, have been show to be necessary for deployment of the sporophyte generation developmental program in *Ectocarpus* (Coelho *et al.*, 2011; Arun *et al.*, 2019). Mutations in either of these genes suppresses the ability of the alga to produce a functional sporophyte, leading to deployment of the gametophyte program at life cycle stages where a sporophyte should normally be produced. In addition, *Ectocarpus* sporophytes have been shown to produce a diffusible factor that can induce sporophyte development in gametophyte initial cells (Arun *et al.*, 2013; Yao *et al.*, 2021). The diffusible factor does not induce life cycle generation switching in *oro* or *sam* mutant gametophyte initial cells, indicating that it acts upstream of ORO and SAM (Arun *et al.*, 2013, 2019).

The genetic pathways that underlie the deployment of the sporophyte and gametophyte developmental programs in brown algae are still poorly understood. Mutations in a small number of genes have been shown to lead to developmental defects in *Ectocarpus* (Macaisne *et al.*, 2017; Godfroy *et al.*, 2017, 2023) but a mutation in the *IMMEDIATE UPRIGHT* gene is the only lesion that specifically affects the development of one of the two generations (Peters *et al.*, 2008). Transcriptomics has been used to identify genes that are differentially expressed between the two generations in *Ectocarpus* (Arun *et al.*, 2019; Lipinska *et al.*, 2019; Bourdareau *et al.*, 2021). These transcriptomic analyses focused on comparisons of adult sporophyte and gametophyte thalli and have allowed the identification of several hundred genes that are differentially expressed between

these two stages of development. However, the analyses were not designed to detect genes that are important during early development and do not provide any information about the kinetics of gene expression over development. In recent years, several detailed studies have generated gene expression data for multiple developmental stages or organs for several different brown algal species (Pearson *et al*., 2019; Shao *et al*., 2019; Shan *et al*., 2020; Zhang *et al*., 2021; Graf *et al*., 2022; Liang *et al*., 2023; Uji *et al*., 2024), including a transcriptomic analyses of early stages of *Dictyota dichotoma* sporophyte development (Bogaert *et al*., 2017). This latter study detected changes in the transcriptome less than one hour after fertilisation, providing evidence for *de novo* transcription in the zygote, and identified a set of genes with diverse functions that were differentially regulated during early sporophyte development.

In the current study, transcriptomic data, recently generated by the Phaeoexplorer project (Denoeud *et al*., 2024), was used to analyse differential gene expression between the adult sporophyte and gametophyte generations of a broad range of brown algae. The proportion of genes that showed generation-biased or generation-specific expression across these two stages was correlated with the level of dimorphism between the two generations indicating that the differentially expressed genes are primarily linked to morphological differentiation. However, analysis of gene ontology terms also identified underlying, life-cycle-related characteristics that have been conserved during evolution, with general classes of gene function being conserved across sporophytes of the ten species, and different general classes of gene function being conserved across the gametophytes. In addition, analysis of transcriptomic data corresponding to multiple stages of the *Ectocarpus* life cycle, generated by combining published RNA sequencing (RNA-seq) data with newly-generated timepoints, identified co-expression modules containing genes with specific expression patterns during life cycle progression. This analysis identified several modules that exhibited marked expression pattern changes during early sporophyte evolution, providing insights into key genetic events during this period. Comparison with a set of gene co-expression modules generated for *D. dichotoma* identified conserved features shared by these two distantly related brown algal species.

Results

Across the brown algal lineage, the proportion of generation-biased genes is correlated with the degree of life cycle dimorphism

RNA-seq data for the adult sporophyte and gametophyte generations of ten different brown algal species (Figure 1A, Table S1) were analysed to obtain a broad overview of generation-biased gene expression across the brown algae. The species analysed had markedly different haploid-diploid life cycles, ranging from sporophyte dominance, through sporophyte-gametophyte isomorphy to gametophyte dominance (Figure S1). As previously observed in a smaller-scale analysis that looked at four different brown algal species (Lipinska *et al*., 2019), the proportion of generation-biased/generation-specific genes (see Materials and Methods for definitions of generation-biased and generation-specific genes) identified in each species was positively correlated with the degree of intergenerational dimorphism (Figure 1B, S1, Table S2). Surprisingly, however, species with strongly dimorphic life cycles had greater numbers of both sporophyte- and gametophyte-biased/specific genes, indicating either that gene downregulation plays an important role in the establishment of dimorphic generations or that there is also cryptic complexification of the more morphologically simple generation.

We also noted that, depending on the species, only between 10% and 24% (Table S2) of genes were expressed during one generation but not the other (defined for this analysis as mean TPM ≥1 for one generation but mean TPM <1 in the other generation), indicating that most genes are expressed during both generations of the life cycle. There is therefore considerable scope for many genes to have functions during both generations of the life cycle. In terms of selection, this observation

157 indicates that most genes are potentially directly exposed to purifying selection during the haploid
158 phase (where there is no effect of masking by a second allele of each locus) and few genes are
159 expressed solely in a diploid context where masking would be most effective.
160
161 **The sporophyte and gametophyte generations express characteristic general functional categories**
162 **of genes**
163
164 To evaluate the degree of conservation of generation-biased/specific gene sets across the ten brown
165 algal species an orthogroup analysis was carried out (Table S3) using Orthofinder (Emms and Kelly,
166 2019). Pairwise comparisons of generation-biased/specific genes that had orthologues in all ten
167 species indicated that the sets of generation-biased/specific genes were poorly conserved across
168 species, even for closely-related species such as the two *Saccharina* spp. (Figure 1C). None of the
169 orthogroups exhibited conserved generation bias across all the ten species. The lack of conservation
170 of generation-biased/specific gene sets across species is in line with observations made in the earlier
171 study that compared four brown algal species (Lipinska *et al.*, 2019). However, despite the poor
172 conservation of generation-biased/specific expression at the individual gene level, analysis of
173 enriched gene ontology terms across the entire generation-biased/specific gene sets from the ten
174 studied brown algae identified distinct sets of enriched terms for both the sporophyte-
175 biased/specific and the gametophyte-biased/specific genes (Figure 2) and the general classes of
176 enriched gene ontology term were conserved for each individual generation across the ten species.
177 For example, the sporophyte-biased/specific gene sets tended to be enriched in genes with predicted
178 functions related to membrane transport and metabolism whereas the gametophyte-biased/specific
179 gene sets tended to be enriched in genes with predicted functions related to flagella biosynthesis
180 and function, protein biosynthesis and DNA-related functions (Figure 2). These analyses identified an
181 underlying similarity between sporophyte generations across species and between gametophyte
182 generations across species, and indicated that these generation-characteristic patterns of gene
183 expression are present even in species where the two generations are isomorphic or nearly
184 isomorphic.
185
186 **Changes in gene expression patterns over the course of the *Ectocarpus* species 7 life cycle reflect**
187 **the cyclic transitions between life cycle stages**
188
189 The above analyses specifically provided information about gene regulation patterns underlying
190 morphological and functional differences between the adult stages of the two generations. To obtain
191 a broader view of gene expression during the life cycle, RNA-seq samples corresponding to multiple
192 stages of the *Ectocarpus* species 7 life cycle were analysed: replicate samples corresponding to two
193 very early stages (24 h and 48 h after gamete release; Figure S2) of sporophyte development were
194 generated and combined with publicly-available samples corresponding to eight other stages of the
195 life cycle (Table S1).
196
197 In a Principal Component Analysis (PCA) the dispersion of the samples corresponding to these ten life
198 cycle stages mirrored the cyclic organisation of the alga life cycle (Figure 3A). Together, the two main
199 axes explained 57% of the observed variability, with adult stages grouping together at one end of the
200 first axis and early stages localised at the other end. The second axis approximately separated the
201 sporophyte and gametophyte phases of the life cycle. The PCA pattern indicated gradual changes in
202 transcriptome content between each stage of the life cycle, so that successive stages possessed
203 overlapping but different transcriptomes.
204
205 **The first day of sporophyte development corresponds to a major shift in the pattern of gene**
206 **expression**
207

208 The PCA also indicated marked differences between the gamete stage and all the other stages of the
209 life cycle (Figure 3A). To further investigate this observation, the Trendy R package (Bacher *et al.*,
210 2018) was used to calculate the fit of segmented regression models to individual gene expression
211 patterns in order to identify individual genes that best matched the overall pattern of regression
212 breakpoints. When this approach was applied to the sporophyte developmental series, a good
213 regression fit ($R^2 > 0.5$) could be calculated for 5,196 genes and 32% of these genes exhibited a
214 change in expression (i.e. a regression breakpoint) during the transition from the gamete stage to the
215 sporophyte initial cell (24 h) stage (Figure 3B), indicating that this transition involves a major shift in
216 the pattern of gene expression.
217
218 To complement the above analysis, DESeq2 (Love *et al.*, 2014) was used to identify genes that were
219 differentially expressed between the free-swimming gamete and the sporophyte initial cell stage.
220 This analysis detected 10,955 differentially expressed genes, corresponding to 4,372 and 6,583
221 significantly up- and down-regulated genes, respectively. These differentially expressed genes
222 represent 58% of the total number of genes in the *Ectocarpus* species 7 genome (Figure 3C). For
223 comparison, when adult sporophytes and gametophytes stage were compared (Figure 1B), 3,726
224 upregulated and 2,577 downregulated genes (35% of the total number of genes overall) were
225 detected. The DESeq2 analysis therefore supported the conclusion that a marked change in gene
226 expression pattern occurred between the free-swimming gamete stage and the sporophyte initial
227 cell stage.
228
229 Interestingly, in the comparison between gametes and the sporophyte initial cell, the mean fold
230 change in transcript abundance for downregulated genes at the transition between free-swimming
231 gamete and initial cell was significantly higher than the mean fold change for genes that were
232 upregulated at this transition (Wilcoxon rank sum test *p*-values $< 2.10^{-16}$; Figure 3D). This observation
233 suggested narrower expression ranges for the downregulated genes and this hypothesis was
234 supported by a comparison of tau values (a measure of breadth of expression) for the downregulated
235 and upregulated genes, which showed that the downregulated genes had significantly higher tau
236 values (Wilcoxon rank sum test *p*-values $< 2.10^{-16}$; Figure S3). A comparison across the ten life cycle
237 stages also showed that 61% of the genes downregulated at the gamete to initial cell transition were
238 most strongly expressed at the gamete stage (data in Tables S4, S5).
239
240 **Analysis of gene co-expression modules indicated coordinated regulation of genes associated with**
241 **several cellular processes**
242
243 To further analyse gene expression patterns over the life cycle, a weighted correlation network
244 analysis (WGCNA) approach (Langfelder and Horvath, 2008) was used to group genes according to
245 their patterns of expression across the ten life cycle stages. Using a cut-off of normalised counts 45
246 (DESeq2 analysis), 16,077 of the 18,370 *Ectocarpus* species 7 genes were classed as being
247 significantly expressed at at least one stage of the life cycle. Of these genes, 14,277 could be assigned
248 to one of 23 gene expression modules, which varied in size from 42 to 2,414 genes (Figures S4, 4,
249 Table S6). The modules were given arbitrary colour names (Figure 4F). The 24th "grey" module
250 groups the 1,800 genes that were not assigned to a co-expression module (Figure 4F, Table S6).
251
252 The 23 gene co-expression modules were analysed for enriched gene ontology (GO) terms (Figures 5
253 and S5). For 11 of the 23 gene co-expression modules, the set of enriched GO terms were sufficiently
254 related to allow a general biological function to be manually assigned to the module (Figure 4A).
255 These modules indicated that at least a proportion of the genes involved in several cellular processes
256 (photosynthesis, DNA modification, flagella biosynthesis/function, transcription and translation) are
257 co-ordinately regulated during the life cycle.
258

259 The PCA and differential expression analyses described above provided evidence for a large-scale
260 modification of the transcriptome during the transition between the gamete and sporophyte initial
261 cell stage. As expected, changes in expression level at this transition strongly influenced the grouping
262 of genes into expression modules (Figure 4F) and several modules were enriched in genes that had
263 been identified as differentially expressed at this first transition (Figure 4C). The following two
264 sections will focus on these modules to further characterise this important early developmental
265 transition.
266
267 **Sporophyte down-regulated gene modules highlighted DNA- and flagella-related functions in**
268 **gametes**
269
270 Seven modules were significantly enriched in genes that were downregulated during the transition
271 from gametes to the sporophyte initial cell (Figure 4C, Table S6). For three of these modules, "pink",
272 "salmon" and "turquoise", the genes were also upregulated during the gametophyte stages (Figure
273 4D). The "pink" module was enriched in gene ontology terms related to nucleosome assembly (Figure
274 S5) and the "salmon" module, which contained a large number of monoexonic genes, was enriched
275 in genes predicted to have DNA-related functions (enriched gene ontology terms included "DNA
276 integration", "DNA recombination", "DNA repair", "DNA helicase" and "telomere maintenance";
277 Figure S5). The "turquoise" module, which had an expression profile very similar to that of the
278 "salmon" module (Figure 4D), was enriched in genes with predicted functions related to the flagella
279 (enriched gene ontology terms included "dynein complex", "cilium", "BBSome", "microtubule-based
280 movement", "axonemal dynein complex assembly", "cilium movement" and "microtubule motor
281 activity"), and therefore presumably important for gamete motility (Figure S5). The upregulation of
282 "turquoise" module genes in gametophytes is probably explained by the production of flagellated
283 gametes in the gametangia of fertile thalli although it is not clear why the genes were also expressed
284 a quite a high level in pre-fertile, adult gametophytes. It is possible that transcripts already
285 accumulate at this stage to prepare for the production of large numbers of gametes at fertility or
286 that some of these genes are also involved in other cellular functions, for example related to the
287 cytoskeleton.
288
289 Cell-wall biosynthesis functions were not significantly enriched in the "turquoise", "salmon" and
290 "pink" modules but these modules contained the majority of annotated genes from two families of
291 carbohydrate-active enzymes (CAZymes), the GT23 family (four genes in the "turquoise" and two
292 genes in the "salmon" module out of ten genes in total) and the PL41 family (nine genes in the
293 "turquoise" module, five genes in the "salmon" module and three genes in the "pink" module out of
294 22 expressed, annotated PL41 genes; Figure S6). The GT23 family is predicted to encode
295 fucosyltransferases, which would transfer fucosyl groups onto chitin oligosaccharides or
296 glycoproteins, and the PL41 family contains mannose-specific alginate lyases (Inoue and Ojima, 2019;
297 Mazéas *et al.*, 2024). While the role of GT23 enzymes in gametes is unclear, it is possible that the
298 polysaccharide depolymerisation action of PL41 lyases may facilitate gamete release from
299 plurilocular sporangia in a manner analogous to the actions of pectate lyases and
300 rhamnogalacturonan lyases during fruit ripening in land plants (Méndez-Yañez *et al.*, 2020; Uluisik
301 and Seymour, 2020; Al-Hinai *et al.*, 2024).
302
303 The remaining four modules that were significantly enriched in genes downregulated during the
304 transition from the gamete to the early sporophyte ("blue", "green", "red" and "grey60") did not
305 exhibit gene upregulation during the gametophyte generation (Figure 4C, D, Table S6). No significant
306 GO term enrichment was detected for the "blue" and "green" modules. The "red" and "grey60"
307 modules were enriched in transcription factors and related GO terms such as "DNA-binding domain"
308 (Figure S5). To investigate this point further a recently established dataset of 325 transcription-
309 associated proteins (TAPs) for *Ectocarpus* species 7 (Denoeud *et al.*, 2024) was enriched with the 90
310 Esv-1-7 domain proteins (Macaisne *et al.*, 2017) from this species (Table S5, Figure S7), as the latter

311 have been hypothesised to function as zinc finger transcription factors (Macaisne *et al.*, 2017), and
312 the expression of these genes analysed in gametes. Transcripts of approximately a third of the genes
313 (147) in this transcription-associated dataset were more abundant in gametes than at the sporophyte
314 initial cell stage (24 h) but the proportion was similar to the proportion for all the genes in the
315 genome indicating that there was not an overall enrichment of the gamete transcriptome in
316 transcription-associated genes.
317
318 Taken together, analysis of the seven modules highlighted the importance of DNA-related functions,
319 including nucleosome assembly and transcription, and flagella-related functions in gametes.
320
321 **Subsets of translation-related genes are upregulated in the sporophyte initial cell but the gamete**
322 **already expresses some translation-related and photosynthesis genes**
323
324 Nine modules were significantly enriched in genes upregulated during the transition between
325 gametes and the sporophyte initial cell (Figure 4C, Table S6). Most of the nine modules could not be
326 clearly associated with a general cellular process but three ("cyan", "magenta" and "greenyellow")
327 were enriched in functions related to translation (Figures 4A, 5). These three modules exhibited very
328 similar expression profiles (Figure 5A) but were enriched in different classes of translation-related
329 gene (Figure 5B-E). The "greenyellow" module contained the RNA polymerase I gene which
330 synthesises rRNA and was enriched in GO terms related to "nucleolus", "small-subunit processome",
331 "ribosome large subunit assembly", "ribosome biogenesis" and "rRNA processing". This module was
332 therefore essentially related to the biosynthesis of the ribonucleic component of the ribosome
333 (Figure 5D). The "cyan" and "magenta" modules were enriched in GO terms such as "tRNA
334 aminoacylation for protein translation", "tRNA processing", "translation initiation" (Figure 5E). These
335 two clusters included 25 of the 49 aminoacyl-tRNA-transferases annotated in the *Ectocarpus* species
336 7 genome, and also included a number of genes related to transcription initiation (Figure 5C).
337 Notably, the "cyan" module included nine eIF3-subunit-encoding genes out of a total of 15 annotated
338 genes in the genome (Figure 5C). Interestingly, the "cyan" and "greenyellow" modules were enriched
339 (p <0.05 clusterProfiler) in genes with a mitochondrial targeting sequence (Figure 4B), whereas the
340 "magenta" module was enriched (p<0.05 clusterProfiler) in genes that encode proteins targeted to
341 the plastid. The plastid-targeted proteins had predicted functions other than photosynthesis (e.g.
342 translation and transport).
343
344 The "cyan", "greenyellow", and "magenta" modules clustered together based on their average
345 expression profiles (Figure 4F), suggesting that the three groups of translation-related functions
346 share some level of co-expression. Taken together, the gene content of these three clusters suggest
347 that there is a marked increase in translation in the initial cell compared to the gamete, both in the
348 cytosolic and the organellar compartments. Importantly, however, not all translation-related genes
349 exhibited marked upregulation during the transition from the gamete to the initial cell stage. For
350 example, the transcripts of the many ribosomal-protein-encoding genes that were grouped in the
351 "purple" module were already present in gametes at relatively high levels (Figures 5B, S8). The
352 ribosomal protein genes are an interesting case because, whilst the majority of these genes were
353 assigned to the "purple" module, corresponding essentially to constitutive expression, a minority of
354 the members of this broad family exhibited more complex expression patterns and were assigned to
355 other modules (Figures 5B, S8). In general, this latter minority of genes tend to encode proteins that
356 are located in close vicinity in the P-stalk within the ribosome (Figure S9). The functional significance
357 of this clustering is unclear but it has been proposed that the P-stalk influences translation fidelity
358 and the pool of mRNAs associated with the ribosome (Wawiórka *et al.*, 2017; Dopler *et al.*, 2024). We
359 also noted that ribosomal protein genes with non-constitutive expression patterns tended to have
360 paralogues that were constitutively expressed (Figure S8). Interestingly, cytosolic and organellar
361 ribosomal protein genes did not exhibit the same patterns of expression with respect to the life

362 cycle, with the genes encoding organellar proteins exhibiting more complex expression patterns (i.e.
363 they were assigned to multiple modules; Figure 5B).
364
365 The "royalblue" module is another example of a module which did not exhibit marked changes in
366 expression between the gamete and the sporophyte initial cell. This module was highly enriched in
367 genes related to photosynthesis or encoding chloroplast-targeted proteins (Figure 4A,B,C). Based on
368 the transcriptomic data, therefore, both cytosolic translation and photosynthesis appear to be
369 processes that are already important at the gamete stage, although it is possible that transcripts
370 related to these processes may accumulate in gametes but be translated at a later stage.
371
372 **Comparative analysis of life-cycle-related gene expression between *Ectocarpus* species 7 and *D.***
373 ***dichotoma***
374
375 To determine whether the developmental and life-cycle-related transcription patterns observed in
376 *Ectocarpus* species 7 corresponded to common, fundamental features that are shared with other
377 brown algae, a comparative analysis was carried out between *Ectocarpus* species 7 and *D.*
378 *dichotoma.* These two species are phylogenetically distant within the brown algal tree (Akita *et al.*,
379 2022). Based on a recent estimate (Choi *et al.*, 2024), their common ancestor dates to about 250
380 Mya. Consequently, if a feature is shared between the two species, this is an indication that it may
381 have been conserved over a significant part of the evolutionary history of the brown algal lineage.
382
383 Replicated transcriptomic data was available for seven stages of the *D. dichotoma* life cycle (Table
384 S1). In a PCA analysis (Figure S10) the adult sporophyte and gametophyte stages clustered together,
385 presumably reflecting the isomorphy between the two generations. Consequently, the distribution of
386 stages in the PCA did not follow the progression of the life cycle, as had been observed for
387 *Ectocarpus* species 7. However, the first dimension clearly separated male gametes from the other *D.*
388 *dichotoma* life cycle stages and the second dimension separated early developmental stages from
389 adult stages. *D. dichotoma* has flagellated male gametes and non-flagellated egg cells. The latter
390 were clustered with early sporophyte stages (zygote and 8h embryo), suggesting that the markedly
391 different gene expression patterns observed in male gametes from the two species compared to
392 other life cycle stages were related to their being actively swimming, flagellated cells rather than
393 being a universal characteristic of all brown algal gametes.
394
395 Life-cycle-related gene expression in *Ectocarpus* species 7 and *D. dichotoma* was compared using two
396 different approaches. The first aimed to determine whether the co-expression patterns of *Ectocarpus*
397 species 7 genes grouped into modules were mirrored by the *D. dichotoma* orthologues of these
398 genes. The second involved independently clustering *D. dichotoma* genes into co-expression modules
399 using life cycle transcriptomic data and then determining whether there were similarities between
400 the modules established for the two species.
401
402 To optimally identify conserved one-to-one orthologues between *Ectocarpus* species 7 and *D.*
403 *dichotoma*, an orthologue analysis was carried out specifically for the two species using Orthofinder
404 (Emms and Kelly, 2019). This approach identified 8,527 one-to-one orthologous relationships
405 between the 18,370 *Ectocarpus* species 7 genes and the 20,583 *D. dichotoma* genes (Table S7). This
406 orthologue dataset was used to compare gene expression patterns in the two species.
407
408 ***D. dichotoma* orthologues of sets of genes from *Ectocarpus* species 7 modules exhibited conserved**
409 **co-expression for some modules that grouped genes involved in the same cellular process**
410
411 To determine whether the co-expression patterns of genes in *Ectocarpus* species 7 modules was
412 conserved in *D. dichotoma,* the *Ectocarpus* species 7 genes in each module were substituted with
413 their *D. dichotoma* orthologues and various parameters, notably the preservation of the density of

414 the module and the preservation of the connectivity, were evaluated (Table S8) using the *D.*
415 *dichotoma* transcriptomic data for the seven different life cycle stages (Table S1). The density
416 preservation of a module was measured by evaluating whether the average correlation for the
417 module was conserved in the second species and whether the module summary profile (module
418 eigengene) still explained a high proportion of the variance after the genes were substituted with
419 orthologues from the second species. Connectivity preservation, on the other hand, determined
420 whether the correlation pattern between the genes was conserved after substitution. Various
421 density and connectivity statistics based on functions in both the WGCNA R package and the NetRep
422 R package were aggregated to estimate conservation of gene co-expression for each *Ectocarpus*
423 species 7 module in *D. dichotoma*.
424
425 Generally, the modules with the best conservation statistics in this analysis were those that had been
426 identified as being highly enriched in *Ectocarpus* species 7 genes with predicted housekeeping
427 functions (Figure 6A). Thus, the "photosynthesis" ("royalblue"), the "ribosome" ("purple"), the
428 "cilium and flagellum" ("turquoise") and various translation-associated ("greenyellow", "cyan", and
429 "magenta") modules all showed a high level of conservation. The expression pattern of the
430 "darkgreen" module was also considered to be conserved in *D. dichotoma* despite the fact only three
431 orthologues were detected. The "darkgreen" module consists principally of genes located within the
432 non-recombining sex-determining region (SDR) of the female (U) and male (V) sex chromosomes
433 (Ahmed *et al.*, 2014) and is therefore a special case because the co-expression pattern is determined
434 not only by gene expression but also by gene presence (i.e. presence of the U or V sex chromosome
435 in gametophytes). The module was considered to be conserved in *D. dichotoma* because the three
436 orthologues are located in the SDR in both species.
437
438 For modules that had good conservation statistics between the two species, *D. dichotoma*
439 orthologues of the *Ectocarpus* species 7 genes that were best correlated with the module eigengene
440 also exhibited a strong correlation with the module eigengene after the *Ectocarpus* species 7 genes
441 had been replaced with the *D. dichotoma* orthologues (Figure 6B). For example, for the "purple" and
442 "royalblue" modules (which had good conservation statistics; Figure 6A) in the top part of Figure 6B,
443 the *Ectocarpus* species 7 genes that were best correlated with the module eigengene are positioned
444 on the left. In the bottom part of the figure the *D. dichotoma* orthologues of these genes are also
445 positioned on the left and they also show strong correlation with the module eigengene. This
446 conservation of correlation with the module eigengene between orthologues was not observed for
447 modules such as "midnightblue" that had poor conservation statistics between the two species
448 (Figure 6B).
449
450 To summarise, this analysis indicated that the co-expression pattern of the genes in a *Ectocarpus*
451 species 7 module following replacement with the *D. dichotoma* orthologues was only conserved for a
452 subset of the modules. The modules that exhibited conservation of co-expression across the two
453 species in this analysis tended to contain sets of genes that functioned in a basic, evolutionarily-
454 conserved cellular process. Moreover, conservation of module co-expression patterns across the two
455 species appeared to be conferred preferentially by orthologues of the *Ectocarpus* species 7 genes
456 that showed the best correlation with the module eigengene.
457
458 **A subset of life-cycle-related gene co-expression modules were conserved between *Ectocarpus***
459 **species 7 and *D. dichotoma***
460
461 For the second approach to compare life-cycle-regulated gene expression in *Ectocarpus* species 7 and
462 *D. dichotoma,* WGCNA was used to define co-expressed gene modules independently for *D.*
463 *dichotoma* using the replicated transcriptomic data for the seven different *D. dichotoma* life cycle
464 stages (Table S1; Figure S4B). The number of modules defined for *D. dichotoma* was lower than the
465 number that had been obtained for *Ectocarpus* species 7 (nine compared with 23; Figure S10, Tables

466 S6, S9, S10), presumably because data was available for fewer life cycle stages and because the *D.*
467 *dichotoma* adult sporophyte and gametophyte generations are isomorphic and therefore have more
468 similar overall gene expression patterns (Figure S10A). As for the *Ectocarpus* species 7 modules,
469 analysis of enriched GO terms (Figure S11) allowed general biological functions to be manually
470 assigned to a subset of the modules (five of the nine modules; Figure S10A).
471
472 Correlation between modules across the two species was assessed based on the number of shared
473 one-to-one orthologues in pairwise comparisons. Fisher's exact test was used to determine whether
474 *Ectocarpus* species 7 and *D. dichotoma* modules shared a greater number of one-to-one orthologues
475 than expected from a random distribution. This analysis identified several pairs of life-cycle-related
476 gene co-expression modules with significantly conserved gene contents between the two species but
477 not all modules were conserved (Figure 6C). As in the first analysis described above, conservation
478 tended to be strongest for *Ectocarpus* species 7 modules that had been manually assigned general
479 functional annotations and which had registered the highest values for module preservation statistics
480 in the first analysis (Figure 6A).
481
482 "Purple" was one of the most strongly conserved *Ectocarpus* species 7 modules: 131 of its 284 one-
483 to-one orthologues were shared with the *D. dichotoma* "blue" module (Figure 6C), with most of the
484 shared orthologues predicted to encode ribosomal proteins. However, the *D. dichotoma* "blue"
485 module exhibited a marked downregulation in male gametes, which was not observed for the
486 *Ectocarpus* species 7 "purple" module. In contrast, the *Ectocarpus* species 7 "turquoise" module,
487 shared 371 (of a total of 1155) one-to-one orthologues with the *D. dichotoma* "green" module,
488 principally with predicted cilium- and flagellum-related functions (Figure 6C,D), and these two
489 modules also exhibited similar life-cycle-related expression patterns, in particular high levels of
490 expression in male gametes. Therefore, both the gene content and the expression patterns of these
491 two modules appear to have been conserved over evolution. Most of the one-to-one orthologues in
492 the translation-related *Ectocarpus* species 7 modules "cyan", "greenyellow" and "magenta"
493 corresponded with genes in the *D. dichotoma* "turquoise" module, consistent with the poorer
494 resolution of the *D. dichotoma* modules (Figure 6C). Nonetheless, all of these modules exhibited a
495 lower level of gene expression in male gametes, indicating conservation of their expression patterns
496 over evolutionary time.
497
498 Taken together, the comparison between *Ectocarpus* species 7 and *D. dichotoma* indicated that there
499 has been partial conservation of life-cycle-related gene expression patterns between the two species,
500 in particular for modules corresponding to clearly-identifiable cellular functions. Moreover, some
501 modules exhibited conservation not only in terms of gene (orthologue) content but also exhibited
502 similar expression patterns over the course of the life cycle, proving further support for the (partial)
503 conservation of life-cycle-related gene expression patterns over time.
504
505 The above analyses provided no evidence that transcription-related modules were conserved,
506 overall, between *Ectocarpus* species 7 and *D. dichotoma* but a more detailed analysis was carried out
507 to determine whether life-cycle-related expression patterns might have been conserved for
508 individual transcription factor genes. For this, 214 transcription factors with one-to-one orthologues
509 in the two species were selected and their expression patterns (normalized expression z-scores)
510 analysed across six life cycle stages that were approximately equivalent between the two species
511 (gamete, zygote, early sporophyte, adult sporophyte, adult male gametophyte and adult female
512 gametophyte; Figure S12, Table S1). High Pearson correlation coefficients were obtained for a subset
513 of the transcription factors but none of the correlations were significant at $p = 0.05$ after correction
514 for multiple testing (Table S11). However, the applied correction was stringent because a large
515 number of orthologous genes were considered so the most strongly correlated transcription factors
516 may nonetheless merit further study in the future. We noted, for example, that all three members of
517 the TALE homeodomain transcription factor family, which includes the life cycle regulators *ORO* and

518 *SAM* (Arun *et al.*, 2019), were among the genes that exhibited high Pearson correlation coefficients in
519 this analysis (Table S11, Figure 6E).
520
521 **Discussion**
522
523 **Subsets of genes with related functions are co-expressed during the life cycle**
524
525 This study analysed replicated RNA-seq samples for ten different stages of the *Ectocarpus* species 7
526 life cycle to provide an overview of life-cycle-related gene expression in this species. Clustering of
527 genes into co-expression modules indicated that subsets of the genes associated with several cellular
528 processes, including transcription, protein synthesis, flagella biosynthesis/function and
529 photosynthesis, are co-ordinately regulated during the life cycle.
530
531 The coordinated expression patterns of the genes in these modules implies coordinated regulation of
532 transcription and/or mRNA stability over the course of the life cycle. The regulatory systems that
533 mediate this coordinated expression are currently unknown for brown algae but information about
534 the mechanisms that co-ordinately regulate these processes in other eukaryote lineages can provide
535 some indications of possible regulators. For example, in *Ectocarpus* species 7, four different modules
536 were enriched in translation-related genes. In other eukaryotic lineages, a large proportion of
537 ribosomal protein genes are regulated by the mTOR/PKA pathway (Martin *et al.*, 2004; Ni and
538 Buszczak, 2023). Interestingly, genes predicted to encode cytosolic and organellar ribosomal proteins
539 were regulated differently in *Ectocarpus* species 7. Note also that this conservation of expression
540 patterns provides additional support for the transfer of the *Arabidopsis* ribosomal protein gene
541 nomenclature (Scarpin *et al.*, 2023) to *Ectocarpus* species 7 genes
542 (https://bioinformatics.psb.ugent.be/orcae/overview/EctsiV2) based on sequence similarity.
543
544 In land plants, photosynthesis-related genes have been shown to be regulated by both light and
545 developmental cues and the regulatory pathways have been characterised. Phytochrome signalling
546 counteracts negative regulation of photosynthesis genes by transcription factors such as
547 PHYTOCHROME-INTERACTING FACTOR (PIF), PIF-LIKE (PIL) and GOLDEN2-LIKE1 (GLK1), which act
548 downstream of various developmentally regulated pathways (Waters *et al.*, 2009; Wang *et al.*, 2017).
549 However, orthologues of these transcription factors have not been found in brown algae and,
550 consequently, coordinated regulation of photosynthetic genes in brown algae, as was observed here
551 for the "royalblue" module, presumably involves a different set of actors.
552
553 As far as flagella- and cilium-related genes are concerned, these organelles are widespread in
554 eukaryotes and the last eukaryotic common ancestor (LECA) probably possessed cilium-related
555 structures (Carvalho-Santos *et al.*, 2011). In Metazoans, two transcription factor families, FOXJ1 and
556 RFX, control the formation of core components of all types of cilia (Choksi *et al.*, 2014). However,
557 although *Saccharomyces cerevisiae* also possesses an *RFX* gene, this family of transcription factors
558 has only been shown to regulate ciliogenesis in metazoans and is not found outside the opisthokonts
559 (Chu *et al.*, 2010). In *Chlamydomonas reinhardtii*, ciliogenesis is under the control of XAP5 (Li *et al.*,
560 2018), a transcription factor that is widely distributed across eukaryotic lineages. Neither *FOXJ1* nor
561 *RFX* have been found in brown algal genomes, but *Ectocarpus* species 7 does possess an *XAP5*
562 homologue (LocusID Ec-05_002220). This gene therefore represents a possible candidate for future
563 analysis of the regulation of this pathway.
564
565 These examples illustrate how candidate regulatory genes may be identifiable for cellular processes
566 that are highly conserved across eukaryotes but candidates are more difficult to identify for modules
567 that group brown-algal-specific genes of unknown function or functions such as the PL41 and GT23
568 gene families that do not have equivalents in other eukaryotic lineages. In some instances, regulatory
569 genes may show similar expression patterns to the genes they regulate as a result of auto-regulation,

570 and therefore be included within a co-expression module, but this will not be the case for all
571 regulators.
572
573 **Identification of marked transcriptome changes during early sporophyte development**
574
575 Analysis of RNA-seq data for multiple developmental stages of *Ectocarpus* species 7 provided a broad
576 overview of gene expression throughout the life cycle, with a particular focus on the early stages of
577 sporophyte development. Progression through the life cycle was correlated with concomitant,
578 progressive changes in the composition of the transcriptome (Figure 3A) and a particularly marked
579 change in composition occurred at the transition from the gamete stage to the initial stage of
580 sporophyte development. Most of the gene co-expression modules identified in this study exhibited
581 changes in transcript abundance at this transition and more than half of the genes in the genome
582 were differentially expressed between the two stages.
583
584 Periods of large-scale changes in transcriptome composition have been observed during early
585 development of both animals and land plants (Xue *et al.*, 2013; Anderson *et al.*, 2017; Vastenhouw *et*
586 *al.*, 2019; Zhao *et al.*, 2019), where they tend to coincide with the maternal-to-zygotic transition
587 (MZT). The MZT corresponds to the switch from reliance on maternal transcripts supplied to the
588 transcriptionally-inactive egg cell to mRNAs produced by transcription of the zygote genome (Tadros
589 and Lipshitz, 2009; Vastenhouw *et al.*, 2019). During the MZT, induction of the expression of genes in
590 the zygote genome, which is referred to as zygotic gene activation (ZGA), coincides with a phase of
591 degradation of maternal transcripts in both animals and land plants. The exact timing of MZT varies
592 across species, occurring rapidly in land plants, only hours after zygote formation (Anderson *et al.*,
593 2017; Chen *et al.*, 2017; Zhao *et al.*, 2019), but considerably later in animals, for example occurring
594 three days after fertilisation in 8-cell human embryos (Xue *et al.*, 2013). However, even in animals, 1-
595 cell stage embryos exhibit a distinct transcriptome pattern (Xue *et al.*, 2013).
596
597 *Ectocarpus* is not oogamous and both male and female gametes are small, flagellated cells that swim
598 actively for a significant part of their lifetime. It therefore seems likely that these cells are already
599 transcriptionally active during the gamete stage, in which case they would not rely solely on
600 maternally-produced transcripts (although this has not yet been investigated experimentally).
601 Consequently, it is not clear whether there is a specific phase of degradation of maternal transcripts
602 in gametes equivalent to the phases of maternal transcript degradation that have been observed at
603 the MZT in land plants and animals. However, the marked change in transcriptome composition
604 during early development is a feature that is shared with animals and land plants, underlining the
605 broad importance of large-scale transcriptional changes during early development.
606
607 In terms of functional categories, fewer genes involved in flagellar function or transcription were
608 expressed after the transition from the gamete stage to the initial stage of sporophyte development.
609 Downregulation of flagellar genes is expected for this transition from a flagellated to a non-
610 flagellated cell. The reduction in the number of expressed transcription factor genes is more
611 surprising but it is likely that the nature of the transcription factor genes expressed or repressed at
612 this stage is more important than the overall number of transcription factor genes expressed. Trends
613 in transcription factor gene up- and down-regulation are not consistent across species, with a
614 decrease in the number of different transcription factor gene transcripts observed in *Arabidopsis*
615 (Zhao *et al.*, 2019) but an increase in rice (Anderson *et al.*, 2017), maize (Chen *et al.*, 2017) and
616 human (Xue *et al.*, 2013), coinciding with the MZT. Moreover, in rice and maize, specific loci that play
617 key roles during embryogenesis such as members of the BABYBOOM and WUSCHEL gene families are
618 upregulated at the MZT/ZGA, supporting the idea that the identity of the specific transcription factor
619 genes expressed is more important than the overall numbers (Anderson *et al.*, 2017; Chen *et al.*,
620 2017). Note that *Ectocarpus* has AP2 domain and homeodomain proteins but no close homologues of

621 the BABYBOOM and WUSCHEL families so it is likely that different transcriptional regulators are
622 involved in regulating development at the equivalent stage in brown algae.
623
624 Analysis of modules that exhibited overall gene upregulation between the gamete and early
625 sporophyte stages identified translation as a general function that was upregulated during this
626 transition. However, the upregulation of these genes does not appear to have corresponded to *de*
627 *novo* induction of translation because a subset of translation-related genes was already expressed at
628 the gamete stage. The overall gene expression pattern is more indicative of a step increase in
629 translation capacity or complexity in the early sporophyte compared to the gamete.
630
631 **Conservation of life-cycle-related gene expression patterns across brown algal species**
632
633 Comparison of generation-biased gene expression between adult gametophyte and sporophyte
634 stages across ten brown algal species identified a strong positive correlation between the degree of
635 dimorphism between generations and the number of GBGs identified per species, indicating that the
636 majority of GBG expression is related directly or indirectly to thallus morphology, at least for the
637 adult stages analysed. Orthologue analysis indicated only weak overlap between GBG sets from
638 different species, supporting an earlier conclusion that there is rapid turnover of GBG sets in brown
639 algae (Lipinska *et al.*, 2019). Interestingly, however, analysis of GO enrichment in GBG sets indicated
640 that several broad functional categories were conserved across gametophyte-biased gene sets,
641 whereas different broad functional categories were conserved across sporophyte-biased gene sets
642 (Figure 2). This observation suggests that the two generations have conserved life-cycle-related
643 functional characteristics that are independent of morphological complexity or the degree of
644 dimorphism between generations.
645
646 The analysis of whole adult individuals to study GBG expression therefore identified some interesting
647 conserved life-cycle-related features but the resolution of this approach is limited because only one
648 sporophyte stage and one gametophyte stage was analysed per species and because, at the adult
649 stage, the data represent an average view of the transcriptomes of multiple different cell types. The
650 comparative analysis of multiple stages of early sporophyte development in *Ectocarpus* species 7 and
651 *D. dichotoma* allowed a more detailed analysis of developmentally regulated gene expression and,
652 notably, showed that there was considerable conservation of co-expressed gene modules between
653 two species, particularly for modules that were enriched in genes involved in evolutionarily-
654 conserved functional categories. Moreover, when the known life cycle regulatory genes *SAM* was
655 analysed, there was clear evidence of conservation of its expression patterns across the two species.
656 These results underline the importance of carrying out detailed transcriptomic analyses to identify
657 and investigate conserved life cycle regulatory pathways.
658
659 **Materials and Methods**
660
661 **Life cycle stages and variants on the sexual cycle**
662
663 Both *Ectocarpus* species 7 and *D. dichotoma* have haploid-diploid life cycles that involve alternation
664 between a sporophyte and a gametophyte generation (Müller, 1967; van den Hoek *et al.*, 1995).
665 During the sexual life cycle, the diploid sporophyte generation produces haploid meio-spores through
666 meiosis. These spores germinate into haploid gametophytes that can be male or female (dioicy).
667 Male and female gametes, produced, respectively, by male and female gametophytes, fuse to
668 produce a diploid zygote, which, in turn, develops into the next sporophyte generation. The zoids
669 (gametes and spores) are the only flagellated stages of the life cycle. In *Ectocarpus* species 7, the
670 germinating zygote undergoes a developmentally symmetrical first division to produce a basal
671 filament, which then branches to establish a basal filament system consisting of round and elongated
672 cells. Once this basal system is established, upright filaments consisting of cylindrical cells grow up

673 into the medium and these filaments bear the sexual structures, plurilocular sporangia and unilocular
674 sporangia (Peters *et al.*, 2008). *Ectocarpus* species 7 also exhibits variations on this basic sexual life
675 cycle, at least in culture (Müller, 1967). For example, parthenogenesis of unfertilised gametes gives
676 rise to haploid partheno-sporophytes. A few hours after release from the plurilocular sporangia,
677 unfertilized free-swimming male gametes attach to the substrate, lose their flagella and acquire a
678 round shape. Upon attachment they start to develop a cell wall. After about two days, the initial cell
679 elongates and divides, producing the first cells of the sporophytic basal filaments. All but one of the
680 sporophyte stages analysed in this study corresponded to partheno-sporophyte samples. Partheno-
681 sporophytes exhibit identical morphology and reproductive functionality to diploid sporophytes and
682 pure samples of early-stage diploid sporophytes are difficult to obtain because of a high level of
683 gamete parthenogenesis in genetic crosses (Coelho *et al.*, 2012a).
684
685 **Publicly available RNA-seq datasets**
686
687 RNA-seq data for the sporophyte and gametophyte generations of the following ten species was
688 recovered from the Phaeoexplorer website (https://phaeoexplorer.sb-roscoff.fr/) or from public
689 databases: *Macrocystis pyrifera, Saccharina latissima, Saccharina japonica, Saccorhiza polyschides,*
690 *Myriotrichia claveaformis, Pylaiella littoralis, D. dichotoma, Sphacelaria rigidula, Ectocarpus* species 7
691 and *Scytosiphon promiscuus*. In addition, RNA-seq data was collected for multiple stages of the *D.*
692 *dichotoma* and *Ectocarpus* species 7 life cycles. All the accession numbers for these data are listed in
693 Table S1.
694
695 **Comparisons of orthologues across multiple brown algal species**
696
697 To compare orthologues across the ten brown algal species analysed for generation-biased gene
698 expression an orthogroup analysis was carried out using Orthofinder (Emms and Kelly, 2019) version
699 2.5.2. Strict selection of only one-to one orthologues did not identify sufficient orthologues (1,038),
700 principally due to gene model fragmentation in the lower quality genome assemblies. A more relaxed
701 selection approach was therefore used, taking into account genome assembly quality. This relaxed
702 approach, which required exactly one orthologue from the best quality assemblies (*D. dichotoma*,
703 *Ectocarpus* species 7, *P. littoralis*, *S. latissima*, *S. promiscuus* and *S. rigidula*), between zero and two
704 orthologues for *M. pyrifera*, zero or one orthologue for *S. japonica*, and any number of orthologues
705 for *S. polyschides* and *M. clavaeformis*, identified 9,317 orthogroups (Table S3). The assumption
706 underlying this approach was that the multiple gene models in the poor-quality genomes
707 corresponded to fragments of a single gene but note that we cannot rule out the possibility that a
708 minority of these groups of genes corresponded to tandem gene duplications. To calculate
709 generation bias when a species possessed more than one gene model in a particular orthogroup,
710 each model was given a score of +1, -1 or 0 if the expression data indicated that they were
711 sporophyte-biased/specific, gametophyte-biased/specific or neither, respectively. The mean of these
712 values was then calculated and the orthologue was classed as sporophyte-biased, gametophyte-
713 biased or unbiased if the value was >0, <0 or 0, respectively.
714
715 **Algal strains and culture conditions**
716
717 *Ectocarpus* species 7 strain Ec32 gametophytes were grown in sterile Provasoli-enriched (0.5x)
718 natural sea water at 13°C under 12h:12h day:night conditions until they reached maturity.
719 Synchronous gamete release was induced by removing excess seawater and incubating in the dark
720 and in the cold for 1 h. Sterile Provasoli-enriched (0.5x) natural sea water (Starr and Zeikus, 1993;
721 Coelho *et al.*, 2012b) was then added and the gametophytes incubated for 30 min to allow gamete
722 release. The medium was filtered through 1 µm cell strainer (pluriSelect, Leipzig, Germany) to
723 eliminate any contaminating gametophytic fragments. The gamete suspension was then diluted to a
724 concentration of 1.5 million cells per mL (A_{450nm} = 0.01) to produce a density of 300 cells per mm² on

725 plastic 150 cm Petri dishes after gamete settlement. After gamete release, the Petri dishes were
726 incubated at 13°C under 12h:12h day:night conditions at a light intensity of 40 µmol.m^{-2}.s^{-1} for 24 or
727 48 h. Cultures were sampled in the late afternoon to ensure homogeneity with regard to circadian
728 rhythms. Sampling was carried out by scraping the bottom of the culture plate with a cell scraper
729 (Sarstedt, Nümbrecht, Germany) after the seawater medium had been removed. The cell suspension
730 was centrifuged at 14000 g for 15 min and the pellet flash-frozen in liquid nitrogen.
731
732 **RNA extraction and RNA-seq sequencing and mapping**
733
734 RNA was extracted using the Macherey Nagel Nucleospin Plant and Fungi kit (Hoerdt, France). Frozen
735 pellets were resuspended in lysis buffer (500 µL of PFL buffer, 40 µL of PFR buffer and 50 µL of 1 M
736 DTT per sample) and the cells were lysed by three 30-second treatments at 7800 rpm in 2 mL "tough
737 micro-organism" lysis tubes (VK05) in a Precellys Evolution homogeniser (Bertin Technologies,
738 Montigny-le-Bretonneux, France), followed by a 5 min incubation at 56°C. RNA extraction followed
739 the manufacturer's instructions except that a DNA digestion step was added after the first wash
740 (digestion on the column with 5 µL of Qiagen DNAse I in 75 µL RDD buffer for 20 s before a second
741 wash with PFW I buffer). The PFW II buffer wash step was carried out three times. RNA was eluted in
742 50 µL of RNAse-free H_2O. RNA-seq libraries were constructed after oligo-dT selection and sequenced
743 by Genewiz (Leipzig, Germany) on an Illumina NovaSeq 6000, using a standard unstranded paired-
744 end protocol to produce a minimum of 50 million reads per condition. Data quality was assessed with
745 FastQC (Andrews, 2016) version 0.11.0 or 0.11.9 and reads were trimmed with Trim Galore (Krueger,
746 2015) version 0.6.5 with parameters --illumina --length 50 --quality 24 --stringency 6 --max_n 3.
747 Genomes were indexed and data was mapped onto the v2 version of the *Ectocarpus* species 7
748 reference genome (Sterck *et al.*, 2012; Cormier *et al.*, 2017) using HISAT2 (Kim *et al.*, 2019) version
749 2.1.0 with default parameters (the parameter --rna-strandedness was specified according to the
750 information in Table S1). The output was converted to bam format and ordered and indexed using
751 the SAMtools (Danecek *et al.*, 2021) version 1.10 functions order and index. Quantification of
752 transcript abundance was carried out using the featureCounts function (Liao *et al.*, 2014) from the
753 Subread package version 2.0.1 on CDS features grouped by Parent or LocusID.
754
755 **Identification of differentially expressed genes**
756
757 Differentially expressed genes were identified using DESeq2 (Love *et al.*, 2014) version 1.34.0 in R
758 version 4.1.2. Genes were considered to be differentially expressed if they had an adjusted
759 (Benjamini-Hochberg false discovery rate) *p*-value of <0.05 and an absolute $\log_2$(FoldChange) greater
760 than 1. Breakpoints in gene expression trends were analysed using the Trendy R package (Bacher *et*
761 *al.*, 2018) version 1.16.0 with the functions trendy (maxK = 3, pvalCut = 0.05) and topTrendy
762 (adjR2Cut = 0.5). DESeq2 version 1.34.0 was also used to calculate normalised counts
763 (NormalisedCounts) using the median of ratios method. Transcripts per kilobase million (TPM) values
764 were calculated from counts of mapped reads using an in-house custom script. Based on the
765 differential expression analyses and the TPM values, genes were classified into six categories:
766 gametophyte-biased (mean gametophyte and mean sporophyte TPM values both 1, log2(fold
767 change) 1, adjusted *p*-value <0.05), sporophyte-biased (mean gametophyte and mean sporophyte
768 TPM values both 1, log2(fold change) -1, adjusted *p*-value <0.05), gametophyte-specific (mean
769 TPM < 1 for the sporophyte and 1 for the gametophyte, log2(fold change) 1, adjusted *p*-value
770 <0.05), sporophyte-specific (mean TPM <1 for the gametophyte and 1 for the sporophyte, log2(fold
771 change) -1, adjusted *p*-value <0.05), unbiased genes (mean gametophyte and mean sporophyte
772 TPM values 1, log2(fold change) <1 or >-1 and/or adjusted *p*-value 0.05) and unexpressed genes
773 (mean gametophyte and mean sporophyte TPM values both <1).
774
775 **Gene ontology and prediction of subcellular localisation**
776

Gene ontology term annotations were extracted from the Interproscan annotation files generated by the Phaeoexplorer consortium (https://phaeoexplorer.sb-roscoff.fr/downloads/; (Denoeud *et al.*, 2024). The subcellular localisation of proteins was predicted by identifying amino-terminal targeting peptides using HECTAR version 1.3 (Gschloessl *et al.*, 2008).

Calculation of breadth of expression and Jaccard indices

Breadth of expression (tau) was calculated using a custom script in R based on the following formula:

$$\tau = (\Sigma(1 - \hat{x}_i))/(n-1)$$

where $\hat{x}_i$ is the expression level of gene i normalized by the maximum expression value across all conditions (mean $\log_2$(NormalisedCounts +1)), and n is the number of conditions.

Jaccard indices were calculated and plotted using vegan version 2.6.8 (https://cran.r-project.org/web/packages/vegan/index.html).

Enrichment analysis

Enrichment of co-expression modules in differentially-expressed genes, predicted subcellular localisations or gene ontology terms were computed using the enricher function from the R package clusterProfiler (Yu *et al.*, 2012) version 4.2.2. *p*-values were adjusted for multiple testing based on the Benjamini-Hochberg false discovery rate.

Identification of modules of co-expressed genes

For both the *Ectocarpus* species 7 and the *D. dichotoma* datasets, raw counts were normalised using the estimateSizeFactors and counts (with option normalized = TRUE) functions from the R package DESeq2 (Love *et al.*, 2014) version 1.34.0. Genes with a normalised count below 45 in all the samples analysed for the relevant species were removed. The normalised counts matrix was then transformed with the log1p (=$\log_2$(x+1)) R function. To fit a scale-free topology model, the soft-thresholding power was selected using the pickSoftThreshold function, and gene modules were built using the blockwiseModules function from the WGCNA R package (Langfelder and Horvath, 2008) version 1.71. For *Ectocarpus* species 7, this function was run with options power = 16, maxBlockSize = 16100 (which yields a topological matrix in one block), minModuleSize = 30, reassignThreshold = 0, mergeCutHeight = 0.2, pamRespectsDendro = FALSE, randomSeed = T, corType = “Pearson”. For *D. dichotoma,* the function was run with power = 18, maxBlockSize = 16000 (which yields a topological matrix in one block), minModuleSize = 30, reassignThreshold = 0, mergeCutHeight = 0.25, pamRespectsDendro = FALSE, randomSeed = T, corType = “Pearson”. Complete module annotation and module membership (MM) scores (or kME, representing the correlation between the gene and the module eigengene) can be found, together with associated *p*-values, in Supplementary Tables S6 and S8. *D. dichotoma* gene module descriptions are in Figure S10B.

Conservation of gene co-expression modules between *Ectocarpus* species 7 and *D. dichotoma*

An orthologue analysis was carried out specifically for *Ectocarpus* species 7 and *D. dichotoma* using Orthofinder (Emms and Kelly, 2019) version 2.5.2 to optimise the identification of one-to-one orthologues for these two species (Table S7). The one-to-one orthologue set generated by this analysis was then used to evaluate module conservation across the two species. The WGCNA package modulePreservation function (networkType = "signed", nPermutations = 20, maxGoldModuleSize = 1000, maxModuleSize = 2500) and the NetRep package (Ritchie *et al.*, 2016) version 1.2.7 modulePreservation function (nPerm=10000, on the WGCNA-computed correlation and TOM matrices) were used to compute module preservation statistics. In addition, the silhouette coefficient for modules was computed using the silhouette_SimilarityMatrix function from the

CancerSubtypes R package (Xu *et al.*, 2017) version 1.20.0 on the correlation matrix. All values can be found in Table S8. The gene correlation heatmap (Figure 6B) was produced using the NetRep (Ritchie *et al.*, 2016) version 1.2.7 plotCorrelation function. The gold module was a random sample of 1,000 *Ectocarpus* species 7 genes that provided a control distribution of gene expression patterns for comparisons with *D. dichotoma* modules. Cross-species module comparisons were visualized as a contingency table (Figure 6C) constructed by interpolating orthologous gene counts between the *Ectocarpus* species 7 and *D. dichotoma* datasets. For each pair of modules, a list of orthologues present in at least one of the two modules was established and a Fisher's exact test was performed on Boolean vectors indicating whether each gene was present in each of the two modules to assess the statistical association between module assignment in both species. The objective was therefore to determine whether each pair of *Ectocarpus* species 7 and *D. dichotoma* modules shared a greater number of one-to-one orthologues than expected from a random distribution. Fisher's exact test was applied using the fisher.test function from the R stats package (version 4.1.2). Cells in the contingency table were colour-coded according to $-\log_{10}(p\text{-value})$.

The contingency table (Figure 6C) was constructed by interpolating gene counts between the *Ectocarpus* species 7 and *D. dichotoma* datasets and using the fisher.test function (alternative = "greater") from the R stats package (version 4.1.2).

Detection of conservation of gene expression patterns between *Ectocarpus* species 7 and *D. dichotoma*

To assess gene expression pattern preservation between *Ectocarpus* species 7 and *D. dichotoma,* a z-score (mean for one condition – mean across all conditions) / standard deviation) was computed from the $\log_2$(NormalisedCounts+1) values for each of the six common timepoints between the *Ectocarpus* species 7 and *D. dichotoma* datasets (Table S1). A Pearson correlation coefficient was then calculated using the R stats package (version 4.1.2) cor.test function (alternative = "greater", method = "pearson").

Manual reannotation of ribosomal protein genes and three-dimensional representation of ribosomal proteins

Ectocarpus species 7 ribosomal proteins were manually annotated using the recent *Arabidopsis thaliana* nomenclature (Scarpin *et al.*, 2023) as a reference (Table S12). *Ectocarpus* species 7 ribosomal proteins were compared with the *A. thaliana* ribosomal protein dataset using BLASTp and the annotations transferred based on the best BLASTp match. To visualise differentially expression in relation to the structure of the ribosome, *Ectocarpus* species 7 ribosomal proteins were mapped onto the *Triticum aestivum* ribosome structure (Protein data bank model 4V7E; (Gogala *et al.*, 2014) and the mapping was visualised using UCSF ChimeraX version 1.9 (Meng *et al.*, 2023).

General data treatment and figure preparation tools

Several R modules were used at multiple stages of the study. These included rtracklayer (Lawrence *et al.*, 2009) version 1.52.1, Tidyverse (Wickham *et al.*, 2019) version 2.0.0, and sjmisc (Lüdecke, 2018) version 2.8.9, which were used to handle and analyse data, and ggplot2 (Wickham *et al.*, 2016) version 3.4.2 and Pheatmap (Kolde, 2019) version 1.0.12, which were used to generate figures.

Data availability

All the new sequence data generated by this study have been deposited in the European Bioinformatics Institute/European Nucleotide Archive (EBI/ENA) database and are publicly available (see Table S1 for details).

881
882 **CRediT authorship contribution statement**
883
884 Conceptualization: P.R., O.G., J.M.C.; Formal analysis: P.R., O.G.; Investigation: P.R., O.G.; Resources:
885 B.N., J.-M.A; Data Curation: P.R., O.G.; Writing - Original Draft: P.R.; Writing - Review & Editing: all
886 authors; Visualization: P.R., O.G.; Supervision: O.G., J.M.C.; Project administration: J.M.C.; Funding
887 acquisition: : J.M.C.
888
889 **Declaration of competing interest**
890
891 The authors declare that they have no known competing financial interests or personal relationships
892 that could have influenced the work reported in this paper.
893
894 **Funding**
895
896 This work was supported by the ANR project Epicycle (ANR-19-CE20-0028-01), the France
897 Génomique National infrastructure project Phaeoexplorer (ANR-10-INBS-09), the CNRS and Sorbonne
898 University. PR acknowledges support from the PhD funding program of École Normale Supérieure de
899 Lyon.
900
901 **Acknowledgments**
902
903 We would like to thank Julia Morales for helpful discussions about ribosomal proteins, Laurence
904 Dartevelle and Elodie Rolland for help with algal cultures, Delphine Scornet, Masakazu Hoshino, Inka
905 Bartsch, Akira F. Peters, Samuel Boscq, Shannon DeVanney for providing seaweed photographs. We
906 are grateful to the Roscoff Bioinformatics platform ABiMS (http://abims.sb-roscoff.fr), which is part
907 of the Institut Français de Bioinformatique (ANR-11-INBS-0013) and BioGenouest network, for
908 providing both help and computing and storage resources.
909
910 **Figures**
911
912 **Figure 1. Generation-biased gene expression across the brown algae**
913 **A.** Cladogram of the brown algae showing the ten species for which generation-biased gene
914 expression was compared. Adapted from (Cock *et al.*, 2014). **B.** Generation-biased gene expression in
915 relation to life cycle dimorphism. Pie diagrams indicating the proportions of sporophyte-specific (dark
916 red), sporophyte-biased (light red), gametophyte-specific (dark blue), gametophyte-biased (light
917 blue) and unbiased (grey) genes in species with different haploid-diploid life cycles ranging from
918 sporophyte-dominant through isomorphic to gametophyte-dominant (indicated by the red and blue
919 wedges). sp., species. **C.** Overlaps (Jaccard index) between sets of gametophyte-biased/specific and
920 sporophyte-biased/specific genes across the ten species.
921
922 **Figure 2. Biological function gene ontology term enrichment in the generation-biased/specific gene**
923 **sets of the ten species**
924 Conserved general functional categories are indicated by coloured boxes. padj, *p*-value adjusted for
925 multiple testing based on the Benjamini-Hochberg false discovery rate.; GA, gametophyte; SP,
926 sporophyte.
927
928 **Figure 3. Gene expression patterns during the *Ectocarpus* species 7 life cycle**
929 **A.** Principal component analysis of the *Ectocarpus* species 7 gene expression across ten life cycle
930 stages. The numbers in circles refer to the differential gene expression analyses illustrated in C and D.
931 Most of the stages analysed consisted entirely of non-flagellated cells with the exception of the
932 gamete stage and mature sporophyte and gametophyte stages, which bear flagellated spores and

933 gametes, respectively, in sporangia and gametangia, respectively. **B.** Percentage changes in gene
934 expression (regression breakpoints) during *Ectocarpus* species 7 sporophyte development (from left
935 to right, transitions between free-swimming male gamete, sporophyte initial cell (24 hours after
936 gamete release), elongating sporophyte initial cell (48 hours after gamete release), sporophyte 2-5
937 cell stage, non-fertile adult sporophyte and fertile sporophyte). **C.** Proportions of differentially
938 expressed genes in the transitions between 1) free-swimming male gamete and sporophyte initial
939 cell stage, and 2) adult sporophyte and gametophyte stages, determined using DESeq2 (Table S1). **D.**
940 Density distribution of the $|\log_2(\text{FoldChange})|$ for upregulated and downregulated genes in the
941 differential gene expression analysis described in C. Dotted lines indicate mean values.
942
943 **Figure 4. Characterisation of gene co-expression modules in *Ectocarpus* species 7**
944 **A.** Functional categories manually assigned to modules based on Gene Ontology term enrichment
945 analysis of each module. **B.** Enrichments in sub-cellular localisations based on HECTAR predictions:
946 mitochondria (small ellipses), plastid (tube shape with thylakoids) and signal peptide/anchor peptide
947 for secreted proteins. Note that HECTAR does not predict nuclear localisation. **C.** Proportion of
948 differentially expressed genes (DESeq2 adjusted p-value < 0.05 and |log2FoldChange| > 1) in each
949 gene module in the transitions between 1) free-swimming male gametes and sporophyte initial cell
950 stage, and 2) adult sporophyte and gametophyte (Table S1). Significant enrichment (indicated by a
951 darker shade of green or orange) means that the proportion of differentially expressed genes in the
952 module was significantly greater (ClusterProfiler adjusted p-value < 0.05) than the proportion for the
953 entire genome. **D.** Average module gene expression profile computed on genes with a WGCNA
954 module MM > 0.86 for, from left to right: free-swimming male gamete, sporophyte initial cell (24
955 hours after gamete release), elongating sporophyte initial cell (48 hours after gamete release),
956 sporophyte 2-5 cell stage, non-fertile adult sporophyte, fertile sporophyte, non-fertile female and
957 male gametophytes, fertile female and male gametophytes developmental stages. **E.** Number of
958 genes in the module positively or negatively correlated with the module eigengene. **F.** Module
959 eigengene dendrogram showing the relationship between module eigengenes.
960
961 **Figure 5. Expression of translation-related genes during *Ectocarpus* species 7 development**
962 **A.** Mean expression profile computed for genes with a WGCNA module MM > 0.86 for (from left to
963 right): free-swimming male gamete, sporophyte initial cell (24 hours after gamete release),
964 elongating sporophyte initial cell (48 hours after gamete release), sporophyte 2-5 cell stage, non-
965 fertile adult sporophyte, fertile sporophyte, non-fertile female and male gametophyte, fertile female
966 and male gametophyte developmental stages in modules "purple", "cyan", "greenyellow",
967 "magenta". **B and C.** Heatmaps showing $\log_2(\text{NormalisedCounts}+1)$ values across the same
968 developmental timepoints as in **A** for manually reannotated ribosomal protein genes corresponding
969 to cytosolic, chloroplast and mitochondrial ribosomal subunits (**B**) and translation-related genes (**C**).
970 Left annotation track: differential expression analysis results for the transitions between 1) free-
971 swimming male gamete and sporophyte initial cell stage, and 2) adult sporophyte and adult
972 gametophyte; right annotation track: WGCNA module colours. **D.** Schematic representation of
973 translation-related functions enriched in the "greenyellow", "purple", "magenta", "cyan" modules.
974 When it was possible to manually assign a general function to a module, the annotation is indicated
975 in brackets after the module name. **E.** Gene ontology terms significantly enriched in the sets of genes
976 clustered within the "purple", "greenyellow", "cyan", and "magenta" modules in *Ectocarpus* species
977 7. Enrichment is indicated as log2 of the ratio of the proportion of genes assigned to the GO term in
978 the module divided by the proportion for the whole genome. CC, cellular component; BP, biological
979 process; MF, molecular function.
980
981 **Figure 6. Conservation of life-cycle-related gene co-expression patterns between *Ectocarpus***
982 **species 7 and *D. dichotoma***
983 **A.** WGCNA density and connectivity median rank statistics indicating the degree of conservation of
984 gene co-expression patterns when of *Ectocarpus* species 7 genes in *Ectocarpus* species 7 co-

985 expression modules were substituted with their *D. dichotoma* orthologues. Manually-assigned
986 general biological functions are indicated in boxes. SDR, sex-determining region. Module size
987 indicates the number of one-to-one orthologues in each module. The modules "darkred" and
988 "darkturquoise" were not included in this analysis because they had only one and zero orthologues,
989 respectively (Table S6). TF, transcription factor; SDR, sex-determining region. **B.** Correlation heatmap
990 comparing three *Ectocarpus* species 7 modules between *Ectocarpus* species 7 and *D. dichotoma*:
991 "midnightblue" (very poor conservation), "purple", and "royalblue" (good conservation). The lower
992 half of the heatmap was calculated based on the expression pattern of the *D. dichotoma* orthologue
993 of each *Ectocarpus* species 7 gene in each module. **C.** Counts of shared one-to-one orthologues
994 between gene co-expression modules defined for *Ectocarpus* species 7 (x-axis) and *D. dichotoma* (y-
995 axis). The colour code represents the $\log_{10}$(*p*-value) for Fisher's exact test (red bar), which was
996 applied to determine whether pairs of modules shared a greater number of one-to-one orthologues
997 than expected from a random distribution. Numbers after the module names indicate the number of
998 one-to-one orthologues in each module. The "darkturquoise" module was not included in this
999 analysis because it contained zero orthologues (Table S6) **D.** Heatmap showing the expression levels
1000 ($\log_2$(NormalisedCounts+1)) of 20 selected one-to-one orthologous flagellum-related genes in
1001 *Ectocarpus* species 7 and *D. dichotoma*. *Ectocarpus* species 7 timepoints: free-swimming male
1002 gamete, sporophyte initial cell (24 hours after gamete release), elongating sporophyte initial cell (48
1003 hours after gamete release), sporophyte 2-5 cell stage, non-fertile adult sporophyte, fertile
1004 sporophyte, non-fertile female and male gametophytes, fertile female and male gametophytes. *D.*
1005 *dichotoma* timepoints: sperm, egg cell, zygote, embryo, adult non-fertile sporophytes, and female
1006 and male gametophytes. **E.** Computed z-score based on $\log_2$(NormalisedCounts+1) values for three
1007 TALE homeodomain transcription factors over six developmental stages shared between *Ectocarpus*
1008 species 7 and *D. dichotoma*, namely sperm, zygote, early sporophyte, non-fertile sporophyte, female
1009 and male gametophyte. The Pearson correlation coefficient between the two expression datasets
1010 (cor) and the associated *p*-value are indicated.
1011
1012 **Supplementary Data**
1013
1014 **Figure S1. Schematic life cycles and photographs of the sporophyte and gametophyte generations**
1015 **of brown algal species analysed in this study illustrating the different degrees of generational**
1016 **dimorphism.**
1017 Size bars indicate the approximate sizes of each generation of each life cycle, providing an indication
1018 of the degree of dimorphism between the two generations. The life cycle and the morphology and
1019 size of the sporophyte and gametophyte generations of *Saccharina japonica* (not shown) are highly
1020 similar to those of *Saccharina latissima*. Photograph credits: *M. pyrifera* sporophyte, Shannon
1021 DeVanney; *S. latissima*, Samuel Boscq (Roscoff Biological Station); *M. clavaeformis*, Akira F. Peters
1022 (Bezhin Rosco); *S. promiscuus* sporophyte, Masakazu Hoshino (Kobe University); *P. littoralis*
1023 gametophyte, Inka Bartsch (Alfred Wegener Institut) and Delphine Scornet (Roscoff Biological
1024 Station); *P. littoralis* sporophyte, Alfred Wegener Institut and Delphine Scornet (Roscoff Biological
1025 Station); *S. polyschides* gametophyte, *M. pyrifera* gametophyte, *E. siliculosus*, Delphine Scornet
1026 (Roscoff Biological Station).
1027
1028 **Figure S2. Light microscopy images of *Ectocarpus* species 7 initial cell and elongating initial cell**
1029 **A.** *Ectocarpus* species 7 strain Ec32 initial cell (settled male Ec32 gamete, 24 h after release). **B.**
1030 *Ectocarpus* species 7 strain Ec32 elongating initial cell (settled male gamete, 48 h after release).
1031 Inverted Leica microscope, magnification: x200, scale bar: 100 µm.
1032
1033 **Figure S3. Breadth of expression (tau) of genes that were differentially expressed, or not, across**
1034 **the transition from gamete to sporophyte initial cell.**
1035 Significantly downregulated and upregulated genes were identified using DESeq2. Dotted lines
1036 indicate mean tau values.

1037
1038 **Figure S4. Hierarchical cluster trees showing co-expression modules identified using WGCNA.**
1039 **A.** *Ectocarpus* species 7. **B.** *D. dichotoma.* Grouped branches correspond to modules, which are
1040 indicated by coloured boxes underneath the tree.
1041
1042 **Figure S5. Enriched GO terms in *Ectocarpus* species 7 gene modules**
1043 Statistically-significant enriched GO terms in *Ectocarpus* species 7 gene modules. Enrichment is
1044 indicated as log2 of the ratio of the proportion of genes assigned to the GO term in the module
1045 divided by the proportion for the whole genome. When it was possible to manually assign a general
1046 function to a module, the annotation is indicated in brackets after the module name. padj, *p*-value
1047 adjusted for multiple testing based on the Benjamini-Hochberg false discovery rate.
1048
1049 **Figure S6. Transcript abundance heatmap for *Ectocarpus* species 7 CAZYme genes**
1050 Heatmaps with log_2(NormalisedCounts+1) for replicate samples of (from left to right) free-swimming
1051 male gamete, sporophyte initial cell (24 hours after gamete release), elongating sporophyte initial
1052 cell (48 hours after gamete release), sporophyte 2-5 cell stage, non-fertile adult sporophyte, fertile
1053 sporophyte, non-fertile female and male gametophyte, fertile female and male gametophyte
1054 *Ectocarpus* species 7 developmental stages for GT23 and PL41 annotated genes. Left annotation
1055 track: differential expression (DEG) analysis results in the transitions between (1) free-swimming
1056 male gamete and sporophyte initial cell stage, and (2) adult sporophyte and gametophyte; right
1057 annotation track: WGCNA module colours.
1058
1059 **Figure S7. Transcript abundance heatmap for *Ectocarpus* species 7 transcription factor genes that**
1060 **have one-to-one *D. dichotoma* orthologues**
1061 Hierarchically clustered heatmap of log_2(NormalisedCounts+1) for 325 *Ectocarpus* species 7 TAP
1062 genes (Denoeud *et al.*, 2024) and 90 EsV1-7 domain genes (Macaisne *et al.*, 2017) for replicate
1063 samples of the following life cycle stages: (from left to right) free-swimming male gamete,
1064 sporophyte initial cell (24 hours after gamete release), elongating sporophyte initial cell (48 hours
1065 after gamete release), sporophyte 2-5 cell stage, non-fertile adult sporophyte, fertile sporophyte,
1066 non-fertile female and male gametophytes, fertile female and male gametophytes. Left annotation
1067 track: differential expression (DEG) analysis results in the transitions between 1) free-swimming male
1068 gamete and initial cell stage, and 2) sporophyte and gametophyte; right annotation track: WGCNA
1069 module colours.
1070
1071 **Figure S8. Transcript abundance heatmap for *Ectocarpus* species 7 ribosomal genes**
1072 Heatmap with log_2(NormalisedCounts+1) for (from left to right) free-swimming male gamete,
1073 sporophyte initial cell (24 hours after gamete release), elongating sporophyte initial cell (48 hours
1074 after gamete release), sporophyte 2-5 cell stage, non-fertile adult sporophyte, fertile sporophyte,
1075 non-fertile female and male gametophyte, fertile female and male gametophyte *Ectocarpus* species 7
1076 developmental stages for ribosomal protein annotated genes. Left annotation track: differential
1077 expression analysis results in the transitions between (1) free-swimming male gamete and
1078 sporophyte initial cell stage, and (2) adult sporophyte and gametophyte; right annotation track:
1079 WGCNA module colours.
1080
1081 **Figure S9. Three dimensional representations of a ribosome illustrating differential expression of**
1082 **ribosomal protein genes**
1083 **A., B.** Lateral views. **C.** Top view. **D.** Bottom view. **E. and F.** Intersubunit views of the small and large
1084 subunit, respectively. Small and large subunit ribosomal proteins are coloured in red and purple,
1085 respectively. Darker colour indicates that the gene encoding a protein was significantly upregulated
1086 between the gamete and sporophyte initial cell stages. Proteins coloured in white are present in the
1087 *Triticum aestivum* ribosome, which was used as a reference, but no equivalent was found in
1088 *Ectocarpus* species 7. RNAs are shown as ribbons, ribosomal RNAs in grey, messenger and transfer

RNAs in green. A, P and T indicate the aminoacyl, peptidyl and exit tRNA binding sites, respectively. En, mRNA entry site; Ex, mRNA exit site; Tu, nascent peptide tunnel exit.

Figure S10. *D. dichotoma* PCA and modules

A. Principal component analysis of *D. dichotoma* gene expression across seven life cycle stages. **B.** Characterisation of *D. dichotoma* gene co-expression modules generated using WGCNA. Left to right: manually-assigned functional categories based on GO term enrichment; number of genes in the module positively or negatively correlated with the module eigengene; average module gene expression profiles for WGCNA modules across sperm (1 h after release), egg cell (15 min after release), zygote (1h after release), embryo (8h after fertilisation), fertile sporophyte, fertile female and male gametophyte life cycle stages; module eigengene dendrogram. The average module gene expression profiles were calculated using genes with a WGCNA MM >0.86.

Figure S11. Enriched GO terms *D. dichotoma* gene modules

Statistically-significant enriched GO terms in *D. dichotoma* gene modules. Enrichment is indicated as log2 of the ratio of the proportion of genes assigned to the GO term in the module divided by the proportion for the whole genome. padj, *p*-value adjusted for multiple testing based on the Benjamini-Hochberg false discovery rate.

Figure S12. Transcript abundance heatmap for one-to-one orthologous transcription factors between *Ectocarpus* species 7 and *D. dichotoma*

Heatmap representing expression of one-to-one orthologous genes from *Ectocarpus* species 7 and *D. dichotoma* presented as the z-score of the $\log_2$(NormalisedCounts+1) for the following equivalent developmental stages in *Ectocarpus* species 7 and *D. dichotoma*: sperm, zygote, early sporophyte, adult sporophyte, female and male gametophyte. The lefthand tracks show Pearson correlation coefficients and $\log_{10}$ Benjamini-Hochberg-adjusted *p*-values (log10 padj).

Table S1. RNA-seq data used in this study

GA, gametophyte; SP, sporophyte; pSP, partheno-sporophyte; GBG, generation-biased genes.

Table S2. Generation-biased and generation-specific gene sets in ten species of brown algae based on comparisons of adult sporophyte and gametophyte generations.

A. Overview of the generation-biased and generation-specific gene sets of each species. **B.** Complete proteomes of the ten species indicating the results of the comparison of adult sporophytes and gametophytes, including $\log_2$(fold change), *p*-value, mean TPM and assigned generation-biased expression class. TPM, transcripts per kilobase million.

Table S3. List of orthogroups for the ten brown algal species analysed for generation-biased gene expression.

The genomes analysed (with ENA accession numbers or links to ORCAE in brackets) correspond to: *Dictyota dichotoma* strain ODC1387m (GCA_964200555), *Ectocarpus* species 7 strain Ec32 (https://bioinformatics.psb.ugent.be/orcae/overview/EctsiV2), *Macrocystis pyrifera* strain P11B4 (GCA_964200385), *Myriotrichia clavaeformis* strain Myr cla04 (GCA_964200105), *Pylaiella littoralis* strain U1.48 (GCA_964200295), *Saccharina latissima* strain SLPER63f7 (GCA_964200175), *Saccharina japonica* strain Ja (https://bioinformatics.psb.ugent.be/orcae/overview/Sacja), *Saccorhiza polyschides* strain SpolBR94m (GCA_964200605), *Scytosiphon promiscuus* strain Ot110409-Otamoi-16-male (GCA_964200365) and *Sphacelaria rigidula* strain Sph rig Cal Mo 4-1-68b (GCA_964200075). The one-to-one orthologues correspond to the 9,317 orthogroups identified using the relaxed criteria described in the Material and Methods.

Table S4. Counts of RNA-seq reads mapped to *Ectocarpus* species 7 genes

This data was used to calculate the gene expression levels reported in Table S4.

1141
1142 **Table S5. Functional and expression-related information for *Ectocarpus* species 7 genes**
1143 List of all *Ectocarpus* species 7 genes with transcript abundance under each of the conditions
1144 analysed, measured as $\log_2$(NormalisedCounts +1), WGCNA module assignment (Colour), WGCNA
1145 module membership (MM) scores and associated *p*-values (pMM) for each gene in each module, the
1146 functional annotation for each gene (description), the manually assigned functional category
1147 (Manual.functional.category), the DESeq2 output for the comparison between free-swimming male
1148 gamete and sporophyte initial cell stage (gamete_initial), and adult sporophyte and gametophyte
1149 (sporophyte_gametophyte) with the corresponding differential expression (DE) annotation, the
1150 HECTAR output for each gene with the predicted targeting category and corresponding scores.
1151
1152 **Table S6. Overview of the gene co-expression modules for *Ectocarpus* species 7 and *D. dichotoma***
1153 The grey modules contain all the genes that could not be assigned to a co-expression module. The
1154 gold module was a random sample of 1,000 *Ectocarpus* species 7 genes that provided a null
1155 distribution of gene expression patterns for the comparisons with *D. dichotoma* modules.
1156
1157 **Table S7. Orthofinder orthogroup analysis of *Ectocarpus* species 7 and *D. dichotoma.***
1158 The genomes analysed (with ENA accession numbers or links to ORCAE in brackets) correspond to:
1159 *Dictyota dichotoma* strain ODC1387m (GCA_964200555) and *Ectocarpus* species 7 strain Ec32
1160 (https://bioinformatics.psb.ugent.be/orcae/overview/EctsiV2).
1161
1162 **Table S8. Conservation of life-cycle-related co-expression modules between *Ectocarpus* species 7**
1163 **and *D. dichotoma***
1164 For each *Ectocarpus* species 7 module: preservation statistics computed by the WGCNA
1165 modulePreservation function (200 permutations), preservation statistics computed by the NetRep
1166 modulePreservation function (10,000 permutations) with the associated $\log_{10}$(*p*-value) (Bonferroni-
1167 corrected for WGCNA), and the silhouette score for each module in *D. dichotoma.* WGCNA -
1168 medianRank statistic, aggregation of the densityMedianRank and connectivityMedianRank statistics;
1169 WGCNA – medianRankDensity.pres, WGCNA density median rank preservation statistic; WGCNA –
1170 medianRankConnectivity.pres, WGCNA connectivity median rank preservation statistic; WGCNA -
1171 propVarExplained.pres, coherence: proportion of module variance explained by the module
1172 eigengene (=summary profile = eigenvector of the 1st principal component across all observations
1173 for every node composing the module); WGCNA – meanSignAwareKME.pres, average node
1174 contribution: average Pearson correlation coefficient to the module's summary profile; WGCNA -
1175 meanSignAwareCorDat.pres, density of correlation structure: how strongly modules are correlated in
1176 the test dataset, average node correlation; WGCNA - meanAdj.pres, average edge weight: average
1177 connection strength between nodes; WGCNA – meanMAR.pres, average module adjacency ratio;
1178 WGCNA: cor.kIM, concordance of intramodular connectivity: similarity of the relative rank of each
1179 nodes' weighted degree (intramodular connectivity) across datasets; WGCNA – cor.kME,
1180 concordance of node contribution: preservation of relative rank of nodes (ordered by Pearson
1181 correlation coefficient to the module's summary profile) across datasets; WGCNA – cor.kMEall;
1182 concordance of node contribution: preservation of relative rank of nodes (ordered by Pearson
1183 correlation coefficient to the module's summary profile) across datasets taking into account the kME
1184 of the gene for all modules; WGCNA - cor.cor, concordance of correlation structure: quantifies how
1185 similar the correlation structure is across datasets; WGCNA – cor.MAR, concordance of module
1186 adjacency ratio: concordance of the ration between the maximum and the minimum adjacency in the
1187 module; WGCNA - separability.pres, separability preservation; NetRep - avg.weight, average edge
1188 weight: average connection strength between nodes; NetRep - coherence, coherence, i. e.
1189 proportion of module variance explained by the module eigengene (=summary profile = eigenvector
1190 of the 1st principal component across all observations for every node composing the module);
1191 NetRep – cor.cor, concordance of correlation structure: quantifies how similar the correlation
1192 structure is across datasets; NetRep - cor.degree, concordance of intramodular connectivity:

similarity of the relative rank of each nodes' weighted degree (intramodular connectivity) across datasets; NetRep - cor.contrib, concordance of node contribution: preservation of relative rank of nodes (ordered by Pearson correlation coefficient to the module's summary profile) across datasets; NetRep - avg.cor, density of correlation structure: how strongly modules are correlated in the test dataset, average node correlation; NetRep - avg.contrib, average node contribution: average Pearson correlation coefficient to the module's summary profile; silhouette.cluster.width, Silhouette coefficient; silhouette.distance.to.average, Silhouette coefficient. The "gold" module was a random sample of 1,000 *Ectocarpus* species 7 genes that provided a control distribution of gene expression patterns for comparisons with *D. dichotoma* modules. The "darkturquoise" module was not included in this analysis because it contained zero orthologues (Table S5).

Table S9. Counts of RNA-seq reads mapped to *D. dichotoma* genes
This data was used to calculate the gene expression levels reported in Table S8.

Table S10. Functional and expression-related information for *D. dichotoma* genes
List of all *D. dichotoma* genes with the $\log_2$(NormalisedCounts+1) under each condition used for the analysis, WGCNA module assignment (Colour), WGCNA module membership (MM) scores and associated *p*-values (pMM) for each gene in each module.

Table S11. Correlation between the expression patterns of orthologous transcription factors in *Ectocarpus* species 7 and *D. dichotoma*
Correlation was evaluated based on comparisons six approximately equivalent stages for the two species (Table S1). The names of the *Ectocarpus* species 7 and *D. dichotoma* genes in each orthogroup are given in Figure S12. padj, *p*-value adjusted for multiple testing based on the Benjamini-Hochberg false discovery rate.

Table S12. Manual re-annotation of the *Ectocarpus* species 7 ribosomal proteins.
The e-values and scores are for BLASTp queries of the *Ectocarpus* species 7 ribosomal proteins against the *Arabidopsis thaliana* ribosomal protein dataset.

References

Ahmed S, Cock JM, Pessia E, Luthringer R, Cormier A, Robuchon M, Sterck L, Peters AF, Dittami SM, Corre E, Valero M, Aury JM, Roze D, Van de Peer Y, Bothwell J, Marais GA, Coelho SM (2014) A Haploid System of Sex Determination in the Brown Alga *Ectocarpus* sp. **Curr Biol** 24:1945–1957.

Akita S, Vieira C, Hanyuda T, Rousseau F, Cruaud C, Couloux A, Heesch S, Cock JM, Kawai H (2022) Providing a phylogenetic framework for trait-based analyses in brown algae: Phylogenomic tree inferred from 32 nuclear protein-coding sequences. **Molecular Phylogenetics and Evolution** 168:107408.

Al-Hinai TZS, Mackay CL, Fry SC (2024) Fruit softening: evidence for rhamnogalacturonan lyase action *in vivo* in ripe fruit cell walls. **Annals of Botany** 133:547–558.

Anderson SN, Johnson CS, Chesnut J, Jones DS, Khanday I, Woodhouse M, Li C, Conrad LJ, Russell SD, Sundaresan V (2017) The Zygotic Transition Is Initiated in Unicellular Plant Zygotes with Asymmetric Activation of Parental Genomes. **Dev Cell** 43:349-358.e4.

Andrews S (2016) FastQC A Quality Control tool for High Throughput Sequence Data. **http://www.bioinformatics.babraham.ac.uk/projects/fastqc/**.

1240 Arun A, Coelho SM, Peters AF, Bourdareau S, Pérès L, Scornet D, Strittmatter M, Lipinska AP, Yao H,
1241 Godfroy O, Montecinos GJ, Avia K, Macaisne N, Troadec C, Bendahmane A, Cock JM (2019)
1242 Convergent recruitment of TALE homeodomain life cycle regulators to direct sporophyte
1243 development in land plants and brown algae. **Elife** 8:e43101.

1244 Arun A, Peters NT, Scornet D, Peters AF, Cock JM, Coelho SM (2013) Non-cell autonomous regulation
1245 of life cycle transitions in the model brown alga *Ectocarpus*. **New Phytol** 197:503–510.

1246 Bacher R, Leng N, Chu L-F, Ni Z, Thomson JA, Kendziorski C, Stewart R (2018) Trendy: segmented
1247 regression analysis of expression dynamics in high-throughput ordered profiling experiments.
1248 **BMC Bioinformatics** 19:380.

1249 Bogaert KA, Beeckman T, De Clerck O (2017) Two-step cell polarization in algal zygotes. **Nat Plants**
1250 3:16221.

1251 Bourdareau S, Tirichine L, Lombard B, Loew D, Scornet D, Wu Y, Coelho SM, Cock JM (2021) Histone
1252 modifications during the life cycle of the brown alga *Ectocarpus*. **Genome Biology** 22:12.

1253 Bringloe TT, Starko S, Wade RM, Vieira C, Kawai H, Clerck OD, Cock JM, Coelho SM, Destombe C,
1254 Valero M, Neiva J, Pearson GA, Faugeron S, Serrão EA, Verbruggen H (2020) Phylogeny and
1255 Evolution of the Brown Algae. **Critical Reviews in Plant Sciences** 39:281–321.

1256 Carney LT, Edwards MS (2006) Cryptic Processes in the Sea: A Review of Delayed Development in the
1257 Microscopic Life Stages of Marine Macroalgae. **Algae** 21:161–168.

1258 Carvalho-Santos Z, Azimzadeh J, Pereira-Leal JB, Bettencourt-Dias M (2011) Evolution: Tracing the
1259 origins of centrioles, cilia, and flagella. **J Cell Biol** 194:165–175.

1260 Chen J, Strieder N, Krohn NG, Cyprys P, Sprunck S, Engelmann JC, Dresselhaus T (2017) Zygotic
1261 Genome Activation Occurs Shortly after Fertilization in Maize. **The Plant Cell** 29:2106–2125.

1262 Choi S-W, Graf L, Choi JW, Jo J, Boo GH, Kawai H, Choi CG, Xiao S, Knoll AH, Andersen RA, Yoon HS
1263 (2024) Ordovician origin and subsequent diversification of the brown algae. **Curr Biol**:S0960-
1264 9822(23)01769-4.

1265 Choksi SP, Lauter G, Swoboda P, Roy S (2014) Switching on cilia: transcriptional networks regulating
1266 ciliogenesis. **Development** 141:1427–1441.

1267 Chu JSC, Baillie DL, Chen N (2010) Convergent evolution of RFX transcription factors and ciliary genes
1268 predated the origin of metazoans. **BMC Evol Biol** 10:130.

1269 Cock JM et al. (2010) The *Ectocarpus* genome and the independent evolution of multicellularity in
1270 brown algae. **Nature** 465:617–621.

1271 Cock JM, Godfroy O, Macaisne N, Peters AF, Coelho SM (2014) Evolution and regulation of complex
1272 life cycles: a brown algal perspective. **Curr Opin Plant Biol** 17:1–6.

1273 Coelho SM, Cock JM (2020) Brown algal model organisms. **Ann Rev Genet** 54:71–92.

1274 Coelho SM, Godfroy O, Arun A, Le Corguillé G, Peters AF, Cock JM (2011) *OUROBOROS* is a master
1275 regulator of the gametophyte to sporophyte life cycle transition in the brown alga
1276 *Ectocarpus*. **Proc Natl Acad Sci USA** 108:11518–11523.

1277 Coelho SM, Scornet D, Rousvoal S, Peters N, Dartevelle L, Peters AF, Cock JM (2012a) Genetic crosses
1278 between *Ectocarpus* strains. **Cold Spring Harb Protoc** 2012:262–265.

1279 Coelho SM, Scornet D, Rousvoal S, Peters NT, Dartevelle L, Peters AF, Cock JM (2012b) How to
1280 cultivate *Ectocarpus*. **Cold Spring Harb Protoc** 2012:258–261.

1281 Cormier A, Avia K, Sterck L, Derrien T, Wucher V, Andres G, Monsoor M, Godfroy O, Lipinska A,
1282 Perrineau M-M, Van De Peer Y, Hitte C, Corre E, Coelho SM, Cock JM (2017) Re-annotation,
1283 improved large-scale assembly and establishment of a catalogue of noncoding loci for the
1284 genome of the model brown alga *Ectocarpus*. **New Phytol** 214:219–232.

1285 Couceiro L, Le Gac M, Hunsperger HM, Mauger S, Destombe C, Cock JM, Ahmed S, Coelho SM, Valero
1286 M, Peters AF (2015) Evolution and maintenance of haploid-diploid life cycles in natural
1287 populations: The case of the marine brown alga *Ectocarpus*. **Evolution** 69:1808–1822.

1288 Danecek P, Bonfield JK, Liddle J, Marshall J, Ohan V, Pollard MO, Whitwham A, Keane T, McCarthy SA,
1289 Davies RM, Li H (2021) Twelve years of SAMtools and BCFtools. **Gigascience** 10:giab008.

1290 Denoeud F et al. (2024) Evolutionary genomics of the emergence of brown algae as key components
1291 of coastal ecosystems. **Cell** 187:6943–6965.

1292 Dopler A et al. (2024) P-stalk ribosomes act as master regulators of cytokine-mediated processes. **Cell**
1293 Available at: https://www.sciencedirect.com/science/article/pii/S0092867424011395
1294 [Accessed November 25, 2024].

1295 Eger AM, Marzinelli EM, Beas-Luna R, Blain CO, Blamey LK, Byrnes JEK, Carnell PE, Choi CG, Hessing-
1296 Lewis M, Kim KY, Kumagai NH, Lorda J, Moore P, Nakamura Y, Pérez-Matus A, Pontier O,
1297 Smale D, Steinberg PD, Vergés A (2023) The value of ecosystem services in global marine kelp
1298 forests. **Nat Commun** 14:1894.

1299 Emms DM, Kelly S (2019) OrthoFinder: phylogenetic orthology inference for comparative genomics.
1300 **Genome Biol** 20:238.

1301 Godfroy O, Uji T, Nagasato C, Lipinska AP, Scornet D, Peters AF, Avia K, Colin S, Mignerot L,
1302 Motomura T, Cock JM, Coelho SM (2017) DISTAG/TBCCd1 Is Required for Basal Cell Fate
1303 Determination in *Ectocarpus*. **Plant Cell** 29:3102–3122.

1304 Godfroy O, Zheng M, Yao H, Henschen A, Peters AF, Scornet D, Colin S, Ronchi P, Hipp K, Nagasato C,
1305 Motomura T, Cock JM, Coelho SM (2023) The *baseless* mutant links protein phosphatase 2A
1306 with basal cell identity in the brown alga *Ectocarpus*. **Development** 150:dev201283.

1307 Gogala M, Becker T, Beatrix B, Armache J-P, Barrio-Garcia C, Berninghausen O, Beckmann R (2014)
1308 Structures of the Sec61 complex engaged in nascent peptide translocation or membrane
1309 insertion. **Nature** 506:107–110.

1310 Graf L, Shin Y, Yang JH, Hwang IK, Yoon HS (2022) Transcriptome analysis reveals the spatial and
1311 temporal differentiation of gene expression in the sporophyte of *Undaria pinnatifida*. **Algal**
1312 **Research** 68:102883.

1313 Gschloessl B, Guermeur Y, Cock J (2008) HECTAR: a method to predict subcellular targeting in
1314 heterokonts. **BMC Bioinf** 9:393.

1315 Inoue A, Ojima T (2019) Functional identification of alginate lyase from the brown alga Saccharina
1316 japonica. **Sci Rep** 9:4937.

1317 Kim D, Paggi JM, Park C, Bennett C, Salzberg SL (2019) Graph-based genome alignment and
1318 genotyping with HISAT2 and HISAT-genotype. **Nat Biotechnol** 37:907–915.

1319 Kolde R (2019) Pheatmap: pretty heatmaps. **R package version** 1:726.

1320 Krueger F (2015) Trim Galore!: A wrapper around Cutadapt and FastQC to consistently apply adapter
1321 and quality trimming to FastQ files, with extra functionality for RRBS data. **Babraham**
1322 **Institute** Available at: https://cir.nii.ac.jp/crid/1370294643762929691 [Accessed October 8,
1323 2024].

1324 Langfelder P, Horvath S (2008) WGCNA: an R package for weighted correlation network analysis.
1325 **BMC Bioinformatics** 9:559.

1326 Lawrence M, Gentleman R, Carey V (2009) rtracklayer: an R package for interfacing with genome
1327 browsers. **Bioinformatics** 25:1841–1842.

1328 Li L, Tian G, Peng H, Meng D, Wang L, Hu X, Tian C, He M, Zhou J, Chen L, Fu C, Zhang W, Hu Z (2018)
1329 New class of transcription factors controls flagellar assembly by recruiting RNA polymerase II
1330 in *Chlamydomonas*. **Proc Natl Acad Sci U S A** 115:4435–4440.

1331 Liang Z, Wang X, Zhang P, Liu W, Wang W, Liu F (2023) Chronological development of the
1332 morphological, physiological, biochemical, and transcriptomic changes provides insights into
1333 the mechanisms of gametogenesis in Saccharina japonica. **J Appl Phycol** 35:785–802.

1334 Liao Y, Smyth GK, Shi W (2014) featureCounts: an efficient general purpose program for assigning
1335 sequence reads to genomic features. **Bioinformatics** 30:923–930.

1336 Lipinska AP, Serrano-Serrano ML, Cormier A, Peters AF, Kogame K, Cock JM, Coelho SM (2019) Rapid
1337 turnover of life-cycle-related genes in the brown algae. **Genome Biol** 20:35.

1338 Love MI, Huber W, Anders S (2014) Moderated estimation of fold change and dispersion for RNA-seq
1339 data with DESeq2. **Genome Biol** 15:550.

1340 Lüdecke D (2018) sjmisc: Data and Variable Transformation Functions. **Journal of Open Source**
1341 **Software** 3:754.

1342 Macaisne N, Liu F, Scornet D, Peters AF, Lipinska A, Perrineau M-M, Henry A, Strittmatter M, Coelho
1343 SM, Cock JM (2017) The *Ectocarpus IMMEDIATE UPRIGHT* gene encodes a member of a novel
1344 family of cysteine-rich proteins with an unusual distribution across the eukaryotes.
1345 **Development** 144:409–418.

1346 Martin DE, Soulard A, Hall MN (2004) TOR regulates ribosomal protein gene expression via PKA and
1347 the Forkhead transcription factor FHL1. **Cell** 119:969–979.

1348 Mazéas L, Bouguerba-Collin A, Cock JM, Denoeud F, Godfroy O, Brillet-Guéguen L, Barbeyron T,
1349 Lipinska AP, Delage L, Corre E, Drula E, Henrissat B, Czjzek M, Terrapon N, Hervé C (2024)
1350 Candidate genes involved in biosynthesis and degradation of the main extracellular matrix
1351 polysaccharides of brown algae and their probable evolutionary history. **BMC Genomics**
1352 25:950.

1353 Méndez-Yañez A, González M, Carrasco-Orellana C, Herrera R, Moya-León MA (2020) Isolation of a
1354 rhamnogalacturonan lyase expressed during ripening of the Chilean strawberry fruit and its
1355 biochemical characterization. **Plant Physiology and Biochemistry** 146:411–419.

1356 Meng EC, Goddard TD, Pettersen EF, Couch GS, Pearson ZJ, Morris JH, Ferrin TE (2023) UCSF
1357 ChimeraX: Tools for structure building and analysis. **Protein Science** 32:e4792.

1358 Müller DG (1967) Generationswechsel, Kernphasenwechsel und Sexualität der Braunalge *Ectocarpus*
1359 *siliculosus* im Kulturversuch. **Planta** 75:39–54.

1360 Ni C, Buszczak M (2023) The homeostatic regulation of ribosome biogenesis. **Semin Cell Dev Biol**
1361 136:13–26.

1362 Pearson GA, Martins N, Madeira P, Serrão EA, Bartsch I (2019) Sex-dependent and -independent
1363 transcriptional changes during haploid phase gametogenesis in the sugar kelp Saccharina
1364 latissima. **PLOS ONE** 14:e0219723.

1365 Peters AF, Scornet D, Ratin M, Charrier B, Monnier A, Merrien Y, Corre E, Coelho SM, Cock JM (2008)
1366 Life-cycle-generation-specific developmental processes are modified in the *immediate*
1367 *upright* mutant of the brown alga *Ectocarpus siliculosus*. **Development** 135:1503–1512.

1368 Ritchie SC, Watts S, Fearnley LG, Holt KE, Abraham G, Inouye M (2016) A Scalable Permutation
1369 Approach Reveals Replication and Preservation Patterns of Network Modules in Large
1370 Datasets. **cels** 3:71–82.

1371 Scarpin MR, Busche M, Martinez RE, Harper LC, Reiser L, Szakonyi D, Merchante C, Lan T, Xiong W,
1372 Mo B, Tang G, Chen X, Bailey-Serres J, Browning KS, Brunkard JO (2023) An updated
1373 nomenclature for plant ribosomal protein genes. **The Plant Cell** 35:640–643.

1374 Shan T, Li Q, Wang X, Pang S (2020) Full-length transcriptome sequencing and comparative
1375 transcriptomic analysis of different developmental stages of the sporophyll in Undaria
1376 pinnatifida (Laminariales: Alariaceae). **J Appl Phycol** 32:2081–2092.

1377 Shao Z, Zhang P, Lu C, Li S, Chen Z, Wang X, Duan D (2019) Transcriptome sequencing of Saccharina
1378 japonica sporophytes during whole developmental periods reveals regulatory networks
1379 underlying alginate and mannitol biosynthesis. **BMC Genomics** 20:975.

1380 Starr RC, Zeikus JA (1993) UTEX-The culture collection of algae at the University of Texas at Austin
1381 1993 list of cultures. **J Phycol** 29 (Suppl.):1–106.

1382 Sterck L, Billiau K, Abeel T, Rouzé P, Van de Peer Y (2012) ORCAE: online resource for community
1383 annotation of eukaryotes. **Nat Methods** 9:1041.

1384 Tadros W, Lipshitz HD (2009) The maternal-to-zygotic transition: a play in two acts. **Development**
1385 136:3033–3042.

1386 Tronholm A, Sansón M, Afonso-Carrillo J, De Clerck O (2008) Distinctive morphological features, life-
1387 cycle phases and seasonal variations in subtropical populations of *Dictyota dichotoma*
1388 (Dictyotales, Phaeophyceae). **Bot Mar** 51:132–144.

1389 Uji T, Kandori T, Mizuta H (2024) Identification of differential gene expression related to reproduction
1390 in the sporophytes of Saccharina japonica. **Front Plant Sci** 15 Available at:

1391 https://www.frontiersin.org/journals/plant-science/articles/10.3389/fpls.2024.1417582/full
1392 [Accessed November 20, 2024].

1393 Uluisik S, Seymour GB (2020) Pectate lyases: Their role in plants and importance in fruit ripening.
1394 **Food Chemistry** 309:125559.

1395 van den Hoek C, Mann DG, Jahns HM (1995) Algae: An Introduction to Phycology. Cambridge:
1396 Cambridge University Press.

1397 Vastenhouw NL, Cao WX, Lipshitz HD (2019) The maternal-to-zygotic transition revisited.
1398 **Development** 146:dev161471.

1399 Wang P, Hendron R-W, Kelly S (2017) Transcriptional control of photosynthetic capacity:
1400 conservation and divergence from *Arabidopsis* to rice. **New Phytol** 216:32–45.

1401 Waters MT, Wang P, Korkaric M, Capper RG, Saunders NJ, Langdale JA (2009) GLK transcription
1402 factors coordinate expression of the photosynthetic apparatus in *Arabidopsis*. **Plant Cell**
1403 21:1109–1128.

1404 Wawiórka L, Molestak E, Szajwaj M, Michalec-Wawiórka B, Mołoń M, Borkiewicz L, Grela P,
1405 Boguszewska A, Tchórzewski M (2017) Multiplication of Ribosomal P-Stalk Proteins
1406 Contributes to the Fidelity of Translation. **Molecular and Cellular Biology** 37:e00060-17.

1407 Wickham H, Averick M, Bryan J, Chang W, McGowan LD, François R, Grolemund G, Hayes A, Henry L,
1408 Hester J (2019) Welcome to the Tidyverse. **Journal of open source software** 4:1686.

1409 Wickham H, Chang W, Wickham MH (2016) Package 'ggplot2.' **Create elegant data visualisations**
1410 **using the grammar of graphics Version** 2:1–189.

1411 Xu T, Le TD, Liu L, Su N, Wang R, Sun B, Colaprico A, Bontempi G, Li J (2017) CancerSubtypes: an
1412 R/Bioconductor package for molecular cancer subtype identification, validation and
1413 visualization. **Bioinformatics** 33:3131–3133.

1414 Xue Z, Huang K, Cai C, Cai L, Jiang C, Feng Y, Liu Z, Zeng Q, Cheng L, Sun YE, Liu J, Horvath S, Fan G
1415 (2013) Genetic programs in human and mouse early embryos revealed by single-cell RNA
1416 sequencing. **Nature** 500:593–597.

1417 Yao H, Scornet D, Jam M, Hervé C, Potin P, Correia LO, Coelho SM, Cock JM (2021) Biochemical
1418 characteristics of a diffusible factor that induces gametophyte to sporophyte switching in the
1419 brown alga *Ectocarpus*. **Journal of Phycology** 57:742–753.

1420 Yu G, Wang L-G, Han Y, He Q-Y (2012) clusterProfiler: an R package for comparing biological themes
1421 among gene clusters. **OMICS** 16:284–287.

1422 Zhang J, Li Y, Luo S, Cao M, Zhang L, Li X (2021) Differential gene expression patterns during
1423 gametophyte development provide insights into sex differentiation in the dioicous kelp
1424 Saccharina japonica. **BMC Plant Biol** 21:335.

1425 Zhao P, Zhou X, Shen K, Liu Z, Cheng T, Liu D, Cheng Y, Peng X, Sun M-X (2019) Two-Step Maternal-to-
1426 Zygotic Transition with Two-Phase Parental Genome Contributions. **Dev Cell** 49:882-893.e5.

1427

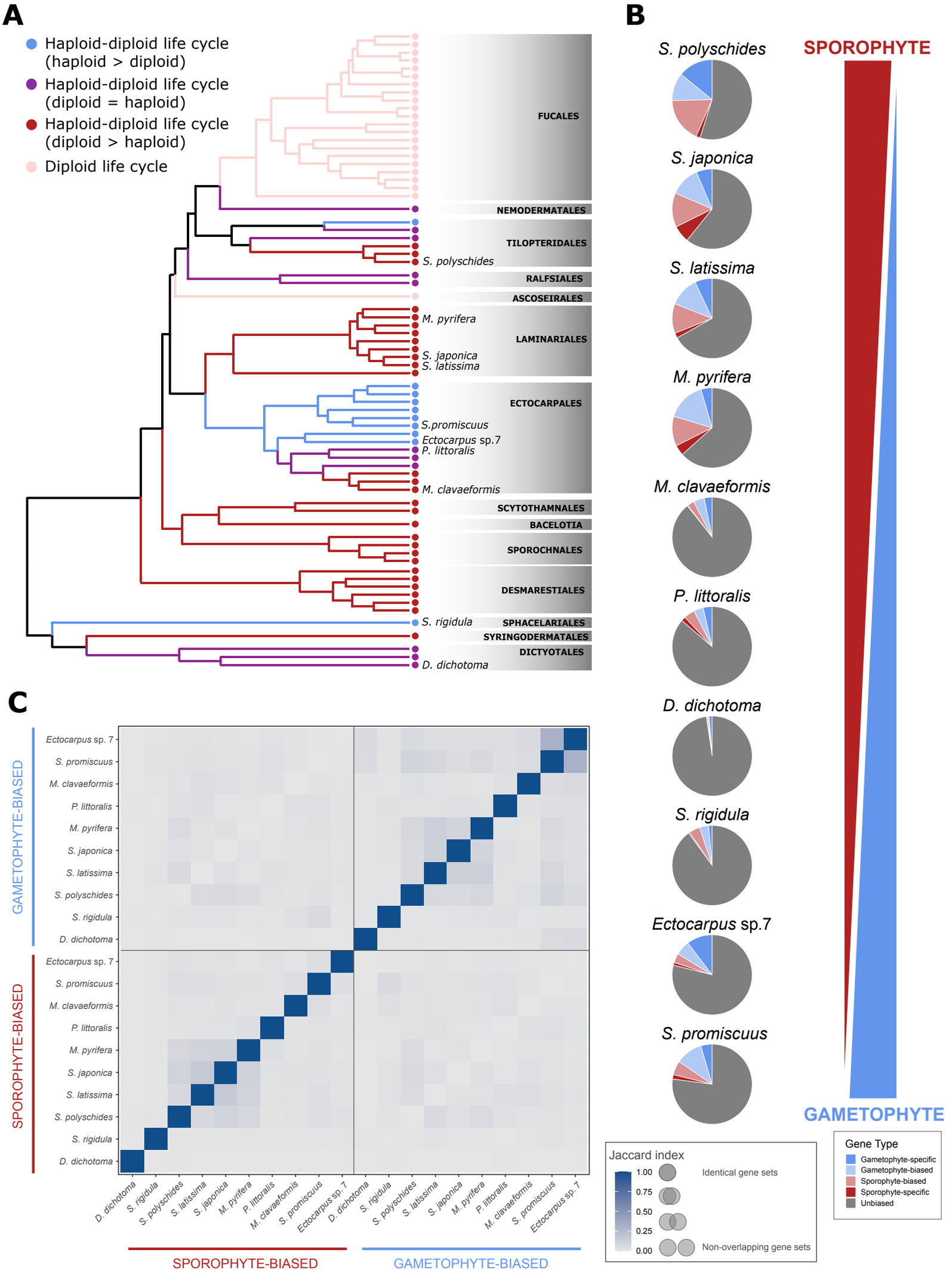
A
Haploid-diploid life cycle (haploid > diploid)
Haploid-diploid life cycle (diploid = haploid)
Haploid-diploid life cycle (diploid > haploid)
Diploid life cycle
FUCALES
NEMODERMATALES
TILOPTERIDALES
S. polyschides
RALFSIALES
ASCOSEIRALES
M. pyrifera
LAMINARIALES
S. japonica
S. latissima
ECTOCARPALES
S.promiscuus
Ectocarpus sp.7
P. littoralis
M. clavaeformis
SCYTOTHAMNALES
BACELOTIA
SPOROCHNALES
DESMARESTIALES
S. rigidula
SPHACELARIALES
SYRINGODERMATALES
DICTYOTALES
D. dichotoma
B
S. polyschides
S. japonica
S. latissima
M. pyrifera
M. clavaeformis
P. littoralis
D. dichotoma
S. rigidula
Ectocarpus sp.7
S. promiscuus
SPOROPHYTE
GAMETOPHYTE
C
GAMETOPHYTE-BIASED
SPOROPHYTE-BIASED
Ectocarpus sp. 7
S. promiscuus
M. clavaeformis
P. littoralis
M. pyrifera
S. japonica
S. latissima
S. polyschides
S. rigidula
D. dichotoma
SPOROPHYTE-BIASED
GAMETOPHYTE-BIASED
Jaccard index
1.00
0.75
0.50
0.25
0.00
Identical gene sets
Non-overlapping gene sets
Gene Type
Gametophyte-specific
Gametophyte-biased
Sporophyte-biased
Sporophyte-specific
Unbiased

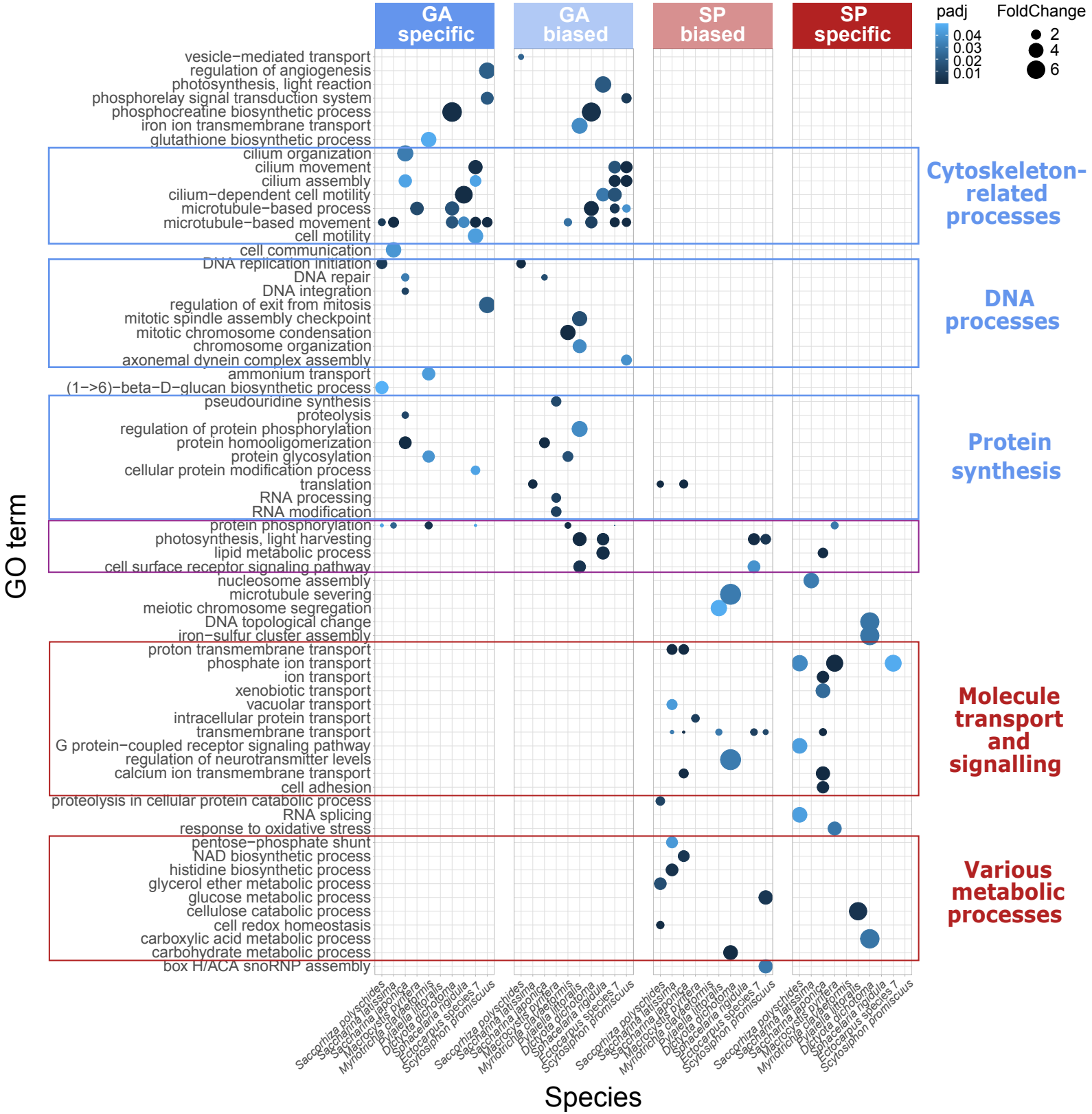
GA specific
GA biased
SP biased
SP specific
padj
0.04
0.03
0.02
0.01
FoldChange
2
4
6
GO term
vesicle−mediated transport
regulation of angiogenesis
photosynthesis, light reaction
phosphorelay signal transduction system
phosphocreatine biosynthetic process
iron ion transmembrane transport
glutathione biosynthetic process
cilium organization
cilium movement
cilium assembly
cilium−dependent cell motility
microtubule−based process
microtubule−based movement
cell motility
cell communication
DNA replication initiation
DNA repair
DNA integration
regulation of exit from mitosis
mitotic spindle assembly checkpoint
mitotic chromosome condensation
chromosome organization
axonemal dynein complex assembly
ammonium transport
(1−>6)−beta−D−glucan biosynthetic process
pseudouridine synthesis
proteolysis
regulation of protein phosphorylation
protein homooligomerization
protein glycosylation
cellular protein modification process
translation
RNA processing
RNA modification
protein phosphorylation
photosynthesis, light harvesting
lipid metabolic process
cell surface receptor signaling pathway
nucleosome assembly
microtubule severing
meiotic chromosome segregation
DNA topological change
iron−sulfur cluster assembly
proton transmembrane transport
phosphate ion transport
ion transport
xenobiotic transport
vacuolar transport
intracellular protein transport
transmembrane transport
G protein−coupled receptor signaling pathway
regulation of neurotransmitter levels
calcium ion transmembrane transport
cell adhesion
proteolysis in cellular protein catabolic process
RNA splicing
response to oxidative stress
pentose−phosphate shunt
NAD biosynthetic process
histidine biosynthetic process
glycerol ether metabolic process
glucose metabolic process
cellulose catabolic process
cell redox homeostasis
carboxylic acid metabolic process
carbohydrate metabolic process
box H/ACA snoRNP assembly
Cytoskeleton-related processes
DNA processes
Protein synthesis
Molecule transport and signalling
Various metabolic processes
Saccorhiza polyschides
Saccharina latissima
Saccharina japonica
Macrocystis pyrifera
Myriotrichia clavaeformis
Dictyota dichotoma
Pylaiella littoralis
Sphacelaria rigidula
Ectocarpus species 7
Scytosiphon promiscuus
Species

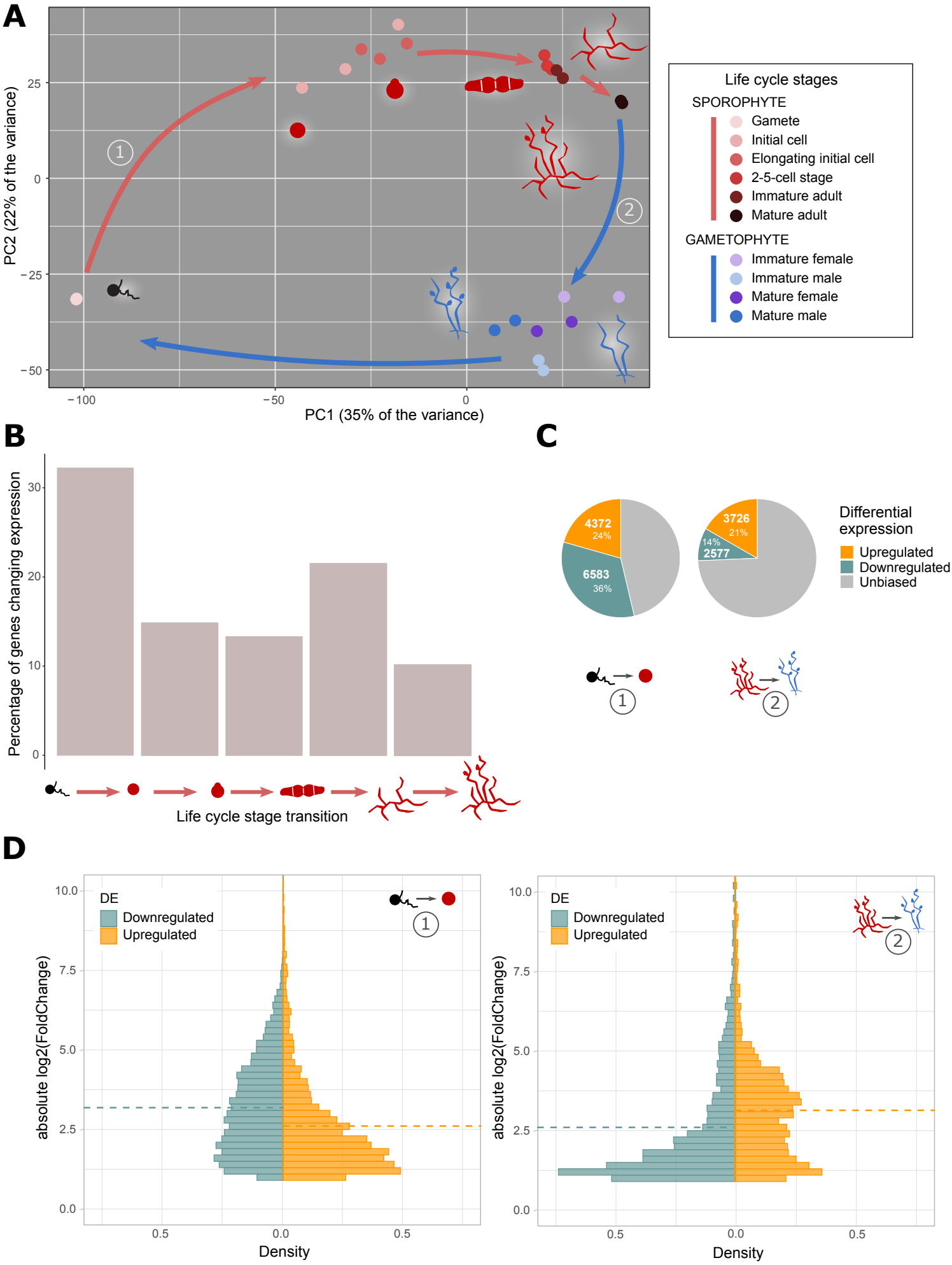
A
PC2 (22% of the variance)
PC1 (35% of the variance)
25
0
−25
−50
−100
−50
0
1
2
Life cycle stages
SPOROPHYTE
Gamete
Initial cell
Elongating initial cell
2-5-cell stage
Immature adult
Mature adult
GAMETOPHYTE
Immature female
Immature male
Mature female
Mature male
B
Percentage of genes changing expression
30
20
10
0
Life cycle stage transition
C
4372
24%
6583
36%
3726
21%
14%
2577
Differential expression
Upregulated
Downregulated
Unbiased
1
2
D
DE
Downregulated
Upregulated
absolute log2(FoldChange)
10.0
7.5
5.0
2.5
0.0
0.5
0.0
0.5
Density
1
2

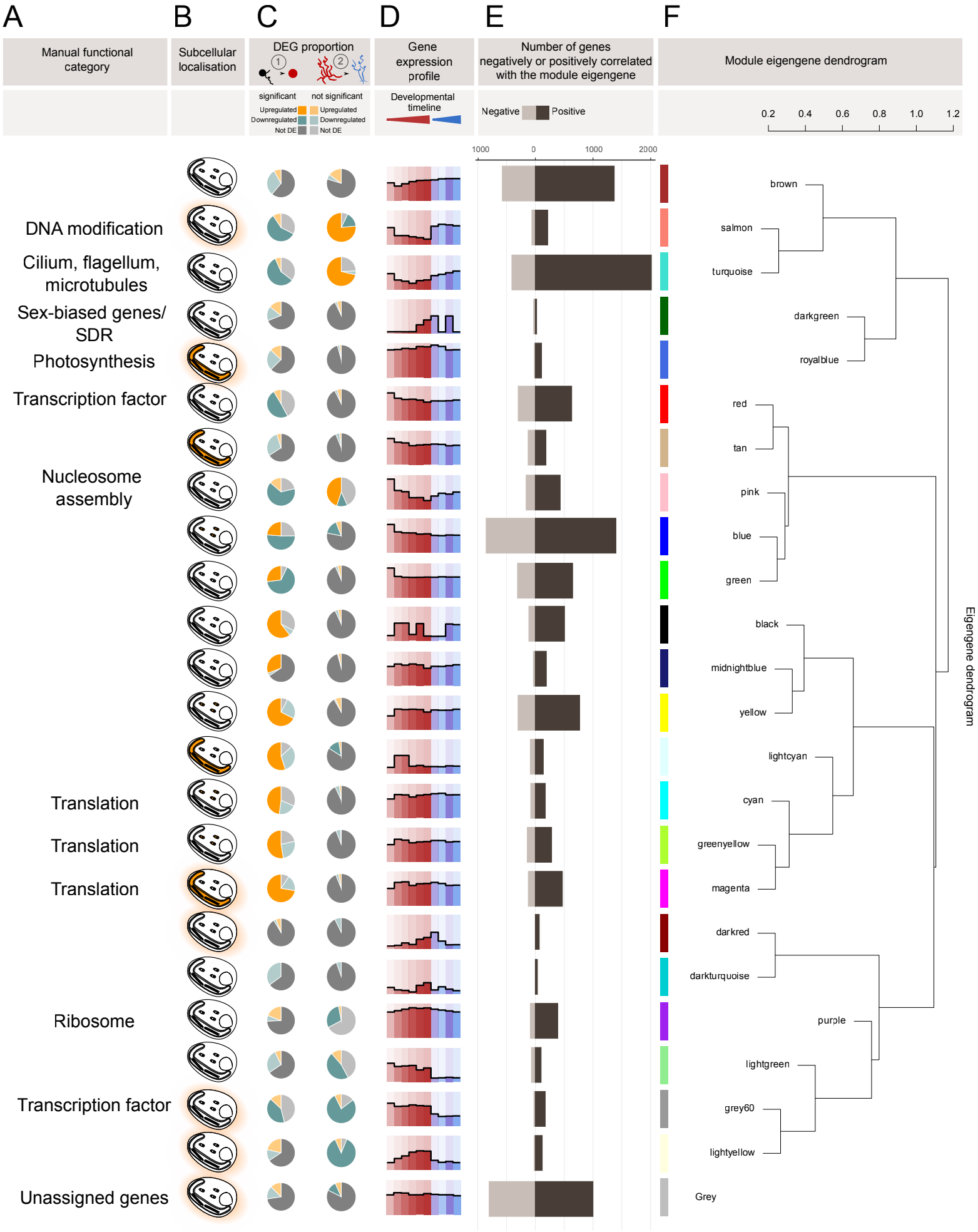
A
B
C
D
E
F
Manual functional category
Subcellular localisation
DEG proportion
Gene expression profile
Number of genes negatively or positively correlated with the module eigengene
Module eigengene dendrogram
significant
not significant
Upregulated
Downregulated
Not DE
Developmental timeline
Negative
Positive
0.2
0.4
0.6
0.8
1.0
1.2
1000
0
1000
2000
DNA modification
Cilium, flagellum, microtubules
Sex-biased genes/ SDR
Photosynthesis
Transcription factor
Nucleosome assembly
Translation
Translation
Translation
Ribosome
Transcription factor
Unassigned genes
brown
salmon
turquoise
darkgreen
royalblue
red
tan
pink
blue
green
black
midnightblue
yellow
lightcyan
cyan
greenyellow
magenta
darkred
darkturquoise
purple
lightgreen
grey60
lightyellow
Grey
Eigengene dendrogram

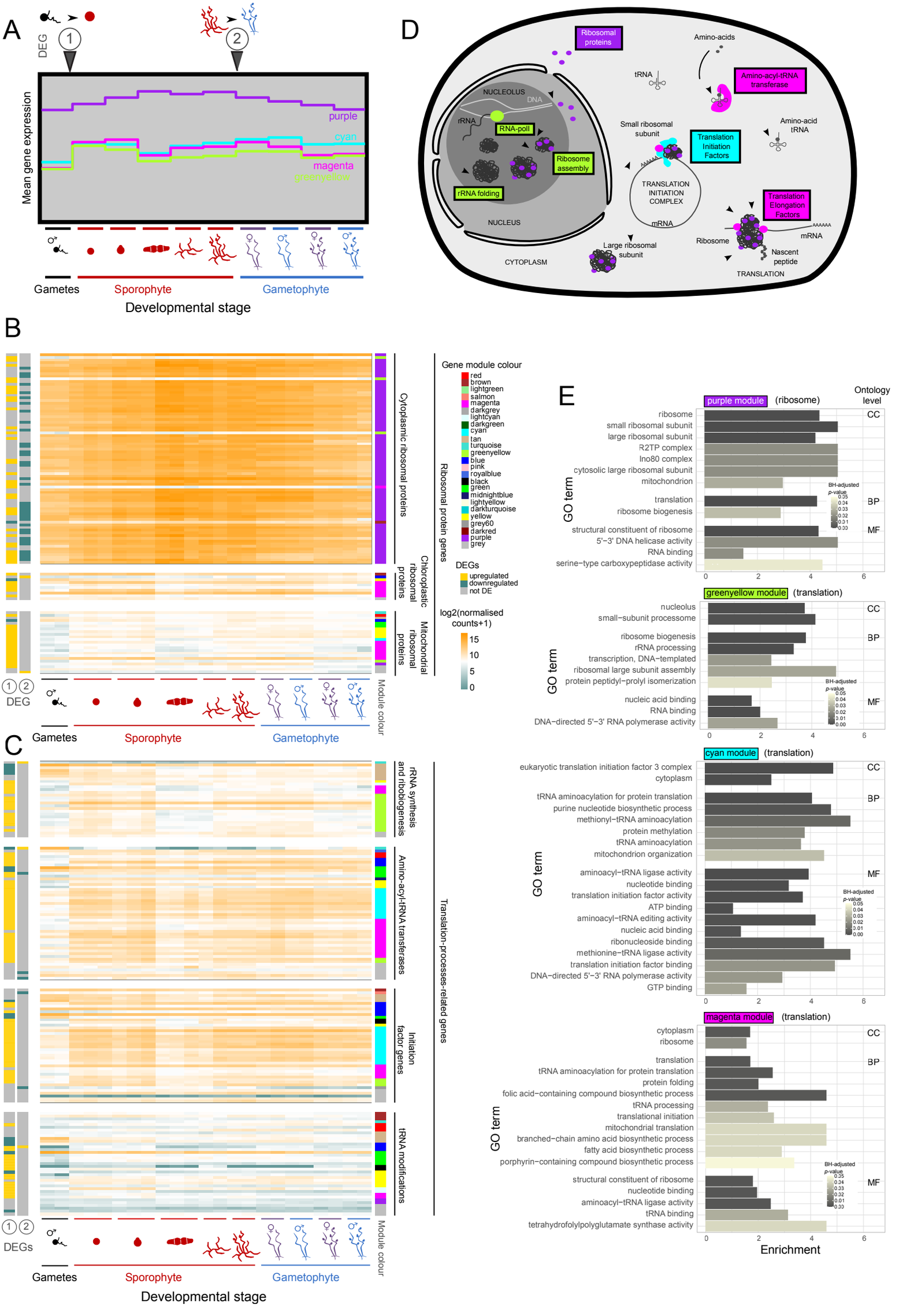
A
DEG
1
2
Mean gene expression
purple
cyan
magenta
greenyellow
Gametes
Sporophyte
Gametophyte
Developmental stage
D
Ribosomal proteins
Amino-acids
tRNA
Amino-acyl-tRNA transferase
NUCLEOLUS
DNA
rRNA
RNA-poll
Small ribosomal subunit
Translation Initiation Factors
Amino-acid tRNA
Ribosome assembly
TRANSLATION INITIATION COMPLEX
rRNA folding
Translation Elongation Factors
NUCLEUS
mRNA
Ribosome
Large ribosomal subunit
Nascent peptide
CYTOPLASM
TRANSLATION
B
Cytoplasmic ribosomal proteins
Chloroplastic ribosomal proteins
Mitochondrial ribosomal proteins
Ribosomal protein genes
Module colour
Gene module colour
red
brown
lightgreen
salmon
magenta
darkgrey
lightcyan
darkgreen
cyan
tan
turquoise
greenyellow
blue
pink
royalblue
black
green
midnightblue
lightyellow
darkturquoise
yellow
grey60
darkred
purple
grey
DEGs
upregulated
downregulated
not DE
log2(normalised counts+1)
15
10
5
0
C
rRNA synthesis and ribobiogenesis
Amino-acyl-tRNA transferases
Initiation factor genes
tRNA modifications
Translation-processes-related genes
DEGs
E
purple module (ribosome)
Ontology level
CC
BP
MF
GO term
ribosome
small ribosomal subunit
large ribosomal subunit
R2TP complex
Ino80 complex
cytosolic large ribosomal subunit
mitochondrion
translation
ribosome biogenesis
structural constituent of ribosome
5'−3' DNA helicase activity
RNA binding
serine−type carboxypeptidase activity
BH-adjusted p-value
greenyellow module (translation)
nucleolus
small−subunit processome
ribosome biogenesis
rRNA processing
transcription, DNA−templated
ribosomal large subunit assembly
protein peptidyl−prolyl isomerization
nucleic acid binding
RNA binding
DNA−directed 5'−3' RNA polymerase activity
cyan module (translation)
eukaryotic translation initiation factor 3 complex
cytoplasm
tRNA aminoacylation for protein translation
purine nucleotide biosynthetic process
methionyl−tRNA aminoacylation
protein methylation
tRNA aminoacylation
mitochondrion organization
aminoacyl−tRNA ligase activity
nucleotide binding
translation initiation factor activity
ATP binding
aminoacyl−tRNA editing activity
nucleic acid binding
ribonucleoside binding
methionine−tRNA ligase activity
translation initiation factor binding
DNA−directed 5'−3' RNA polymerase activity
GTP binding
magenta module (translation)
cytoplasm
ribosome
translation
tRNA aminoacylation for protein translation
protein folding
folic acid−containing compound biosynthetic process
tRNA processing
translational initiation
mitochondrial translation
branched−chain amino acid biosynthetic process
fatty acid biosynthetic process
porphyrin−containing compound biosynthetic process
structural constituent of ribosome
nucleotide binding
aminoacyl−tRNA ligase activity
tRNA binding
tetrahydrofolylpolyglutamate synthase activity
Enrichment

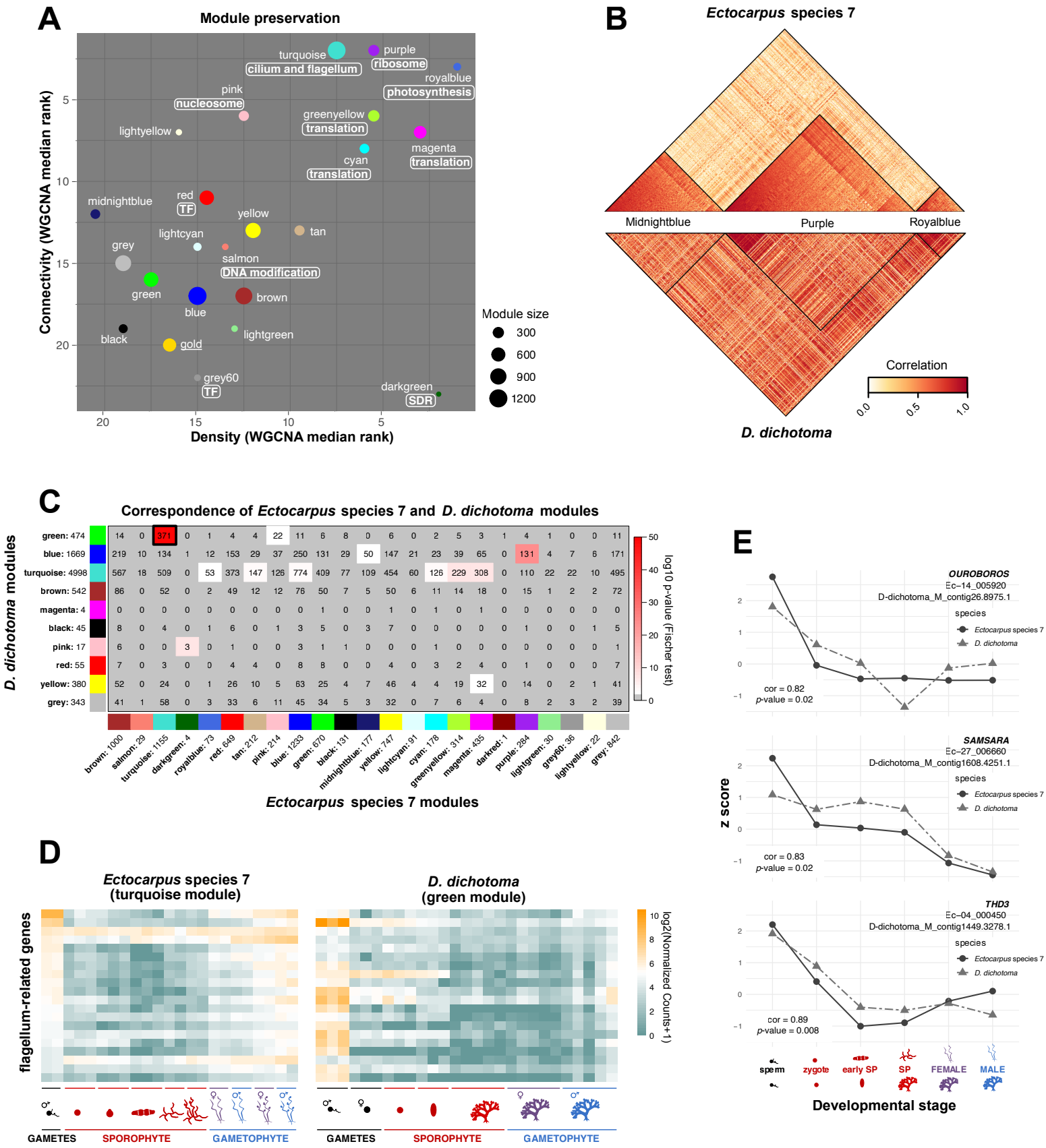
A
Module preservation
Connectivity (WGCNA median rank)
Density (WGCNA median rank)
turquoise
cilium and flagellum
purple
ribosome
royalblue
photosynthesis
pink
nucleosome
greenyellow
translation
lightyellow
magenta
translation
cyan
translation
midnightblue
red
TF
yellow
tan
lightcyan
grey
salmon
DNA modification
green
brown
blue
black
lightgreen
gold
grey60
TF
darkgreen
SDR
Module size
300
600
900
1200
B
Ectocarpus species 7
Midnightblue
Purple
Royalblue
Correlation
0.0
0.5
1.0
D. dichotoma
C
Correspondence of Ectocarpus species 7 and D. dichotoma modules
D. dichotoma modules
green: 474
blue: 1669
turquoise: 4998
brown: 542
magenta: 4
black: 45
pink: 17
red: 55
yellow: 380
grey: 343
brown: 1000
salmon: 29
turquoise: 1155
darkgreen: 4
royalblue: 73
red: 649
tan: 212
pink: 214
blue: 1233
green: 670
black: 131
midnightblue: 177
yellow: 747
lightcyan: 91
cyan: 178
greenyellow: 314
magenta: 435
darkred: 1
purple: 284
lightgreen: 30
grey60: 36
lightyellow: 22
grey: 842
log10 p-value (Fischer test)
Ectocarpus species 7 modules
D
Ectocarpus species 7
(turquoise module)
D. dichotoma
(green module)
flagellum-related genes
log2(Normalized Counts+1)
GAMETES
SPOROPHYTE
GAMETOPHYTE
E
OUROBOROS
Ec–14_005920
D-dichotoma_M_contig26.8975.1
species
Ectocarpus species 7
D. dichotoma
cor = 0.82
p-value = 0.02
SAMSARA
Ec–27_006660
D-dichotoma_M_contig1608.4251.1
cor = 0.83
p-value = 0.02
THD3
Ec–04_000450
D-dichotoma_M_contig1449.3278.1
cor = 0.89
p-value = 0.008
z score
sperm
zygote
early SP
SP
FEMALE
MALE
Developmental stage